ADDIS ABABA UNIVERSITY

SCHOOL OF GRADUATE STUDIES

INSTITUTE OF TECHNOLOGY
ELECTRICAL AND COMPUTER ENGINEERING DEPARTMENT

BANDWIDTH AND GAIN PERFORMANCE COMPARISON OF RECTANGULAR-PATCH MICROSTRIP ANTENNA (RMSA) AND COPLANAR WAVEGUIDE (CPW) RECTANGULAR-PATCH ANTENNA

By: ABIY BEKELE

A thesis submitted to the school of Graduate Studies of Addis Ababa University in partial fulfillment of the requirements for the Degree of Masters of Science in Electrical Engineering (Communication Engineering)

Advisor: Dr. -Ing. Mohammed Abdo

January 2011

Addis Ababa, Ethiopia

ADDIS ABABA UNIVERSITY

SCHOOL OF GRADUATE STUDIES

INSTITUTE OF TECHNOLOGY
ELECTRICAL AND COMPUTER ENGINEERING DEPARTMENT

BANDWIDTH AND GAIN PERFORMANCE COMPARISON OF RECTANGULAR-PATCH MICROSTRIP ANTENNA (RMSA) AND COPLANAR WAVEGUIDE (CPW) RECTANGULAR-PATCH ANTENNA

By: ABIY BEKELE

Approval by Board of Examiners:

Chairman (*Dept. Graduate Committee*)	**Signature**
Advisor	**Signature**
Internal Examiner	**Signature**
External Examiner	**Signature**

Declaration

I, the undersigned, hereby declare that this thesis is my original work and has not been presented for a degree in any other university, and that all sources of material used for the thesis have been duly acknowledged.

Name: Abiy Bekele

Signature: _____

Place: Addis Ababa

Date: _____

This thesis has been submitted for examination with my approval as a university advisor.

Name: Dr.-Ing. Mohammed Abdo

Signature: _____

Place: Addis Ababa

Date: _____

CHAPTER 1

Thesis Overview

1.1 Introduction

In today's world, microstrip antenna and coplanar waveguide patch antenna are used in all wireless communication such as cellular telephony, satellite, portable personal communication, aircraft, spacecraft, and missile applications. The growth and popularity of wireless application is quite dominant because of its mobility, the demand for high speed transmission of large data, customer request for multi-media service, and the need for new technologies, as well. This shows that there is a large investment that has been put in to wireless communication by major companies in the telecommunication industry.

WLAN is one part of the investment that gains an increase in its usage because it provides high quality of services with low cost to more users. The *IEEE 802.11* workgroup currently use three frequency ranges 2.4 GHz, 3.6 GHz and 5 GHz for *WLAN* technologies. Each range is divided into a multitude of channels. Countries apply their own regulations to both the allowable channels, allowed users and maximum power levels within these frequency ranges [1].

According to the *IEEE 802.11n* standard, *WLAN* technologies operating at 5 GHz frequency range has the frequency spectrum ranges from 5.15 GHz to 5.85 GHz (i.e.; 5.15–5.25, 5.25–5.35, and 5.75–5.85 GHz) to construct twelve non-overlapping 20 MHz channels or as many as six non-overlapping 40 MHz channels. *IEEE 802.11n* also takes advantage of new worldwide regulatory changes making the 5.47–5.75 GHz band available for ***unlicensed*** *WLAN* use [2]. Therefore, in this thesis *RMSA* and *CPW-RPA* operating at resonant frequency of 5.5 GHz have been designed.

1.2 Motivation

Future wireless communication systems will require significantly higher data rates and reduction in costs per transmitted bit. The demands on data rate, link quality, spectral efficiency, mobility, flexibility and complexity cannot be met with conventional wireless systems. One of the factors is the *growth of bandwidth requirement* in order to provide reliable and good quality of voice, multimedia, and data services [3].

Despite their advantages; low profile, light weight, low volume and easy fabrication and so on, as compared to the conventional microwave antennas, narrow bandwidth and low gain are the two major limitations of microstrip and coplanar waveguide antennas. The *compact configuration* of *MSA* and *CPWA* is the main factor to these limitations. The smaller the antenna, either the operation bandwidth or the antenna efficiency (gain) will be decreased. However, in comparison with *MSA*, *CPWA* has higher bandwidth but lower gain. Therefore, in this thesis bandwidth enhancement has become a major consideration in the design *MSA*.

1.3 Statement of the Problem

In wireless communication system antenna is the key element to establish communication link and cover wide frequency range. To ensure efficient and reliable connectivity in a *WLAN* system and to utilize fully the frequency spectrum of a 5 GHz band based on *IEEE 802.11n* standard, *MSA* should have broader bandwidth [1, 2].

However, inherent narrow bandwidth of a few percent is one of the principal disadvantages of *MSA* in its basic form. This is a limitation for the growth of future bandwidth requirement. That is why this thesis is dealing with bandwidth enhancement of the *conventional MSA*.

1.4 Objective

The general objective of this thesis is to review the fundamental principles about *MSA* and *CPWA*. The specific objectives are to design: *conventional RMSA*, *BW-Enhanced RMSA* by using the technique called “lowering the total quality factor”, and to design *CPW-RPA*. Finally, we will compare their *bandwidth* and *gain* performance.

1.5 Literature Review

Throughout the years after microstrip radiators was first proposed by Deschamps in 1953 and the first practical *MSA* were fabricated in 1970s [6], several authors have dedicated their time to create new designs with variation to the original antenna design. That is, they have come with the property either wider bandwidth or multiple-frequency operation or size reduction, and so on. Some of the researches conducted by others in the area of bandwidth enhancement of *MSA* are:

- "*Bandwidth Enhancement of A Microstrip Antenna Using Negative Inductance As Impedance Matching Device*", by Adnan Kaya, Selcuk Kilinc, E. Yesim Yuksel, and Ugur Cam [19].
    - ✓ *BW enhancement of MSA is achieved by using a floating negative-inductor circuit as a compensation (matching) network;*
    - ✓ *The simulation results show that compensation network can improve the bandwidth from 17.21% to 32.67%.*
- "*Bandwidth Enhancement for Microstrip Antenna in Wireless Applications*", by RSA Raja Abdullah, D Yoharaaj and A Ismail [20].
    - ✓ *BW enhancement of MSA is achieved by using Identical Dual-Patch Microstrip Antenna with Air-Gap (IDMA);*
    - ✓ *This technique takes the advantage of using the air gap to increase the total thickness of the microstrip antenna which is essential for bandwidth enhancement;*
    - ✓ *By using this technique, a bandwidth enhancement of about 11% has been achieved.*

Another interest area of this thesis is coplanar waveguide patch antenna. *CPW* was originally proposed by C. P. Wen from *RCA* Laboratory in 1969. The term coplanar lines is used for those transmission line where all the conductors are in the same plane; namely, on the top surface of the dielectric substrate. The original design assumed the adjacent ground strip widths and

dielectric thickness were infinite. Over the years, many inventors modified the design to achieve superior attenuation and dispersion characteristics for meeting specific applications. Some of the researches conducted by others related to this area are:

- "*Electric Field in Coplanar Patch Antennas (CPA): Simulation and Measurement*", by K. Li, C. H. Cheng, T. Matsui and M. Izutsu [31].

  This paper revealed that the coplanar waveguide patch antenna behaves more like a microstrip patch antenna rather than a loop slot antenna based on intensive electromagnetic field simulations of the structure and experiments on the antenna. Particularly:

  - ✓ *The resonant frequency of the antenna is primarily determined by the patch length (L) of about a half guided wavelength instead of the total loop size;*
  - ✓ *Electromagnetic simulation also demonstrated the similar distribution of the electric fields around the slots as the distribution around the microstrip patch edges;*
  - ✓ *Similar tendency of the input impedance versus the length (L) of the patch has been also observed. This makes possible to realize an impedance matching by only adjusting the width (W) of the patch*.

- "*Broad-Band Double-Layered Coplanar Patch Antennas With Adjustable CPW Feeding Structure*," K. F. Tong, K. Li, T. Matsui, and M. Izutsu [34].

  - ✓ *This paper presented the double-layered coplanar patch antennas of enhanced impedance bandwidth and adjustable conductor backed coplanar waveguide feed lines;*
  - ✓ *The proposed structure retains the advantage of laying the coplanar patch and CPW feed line on the same surface, which makes direct integration with other devices easier;*
  - ✓ *In addition, the substrate thickness of the radiating patch can be adjusted to achieve a wider impedance bandwidth while the dimensions of the CPW feed line are kept unchanged.*

However, for this thesis I have implemented one of the techniques called "lowering the total quality factor" to enhance the bandwidth of the conventional *RMSA*. This has also been achieved by increasing the substrate height and patch width, but keeping the dielectric constant the same.

1.6 Thesis Outline

The thesis is organized as:

Chapter 1: This chapter gives the thesis overview.

Chapter 2: Presents the basic concept of microstrip antenna, patch shapes, its advantages and disadvantages, its principles of operation, feeding techniques, methods of analysis and antenna main parameters.

Chapter 3: This chapter presents an introduction to the coplanar waveguide antenna, its advantages and disadvantage over convention microstrip antenna, its methods of analysis.

Chapter 4: This chapter describes the design of conventional and bandwidth-enhanced rectangular microstrip antenna and coplanar waveguide rectangular-patch antenna.

Chapter 5: The simulation result obtained, the comparison between theoretical and simulation results and the comparison of bandwidth and gain among the three antennas are discussed here.

Chapter 6: In this last chapter the conclusion and the recommendation for future work is Presented

CHAPTER 2

Microstrip Antenna

2.1 The Basic of Microstrip Antenna

Microstrip antennas are one of the most widely used types of antennas in the microwave frequency region, and they are often used in the millimeter-wave frequency range as well. Below approximately 1 GHz, the size of a microstrip antenna is usually too large to be practical and other type of antennas such as wire antennas dominate. Microstrip antennas consist of a very thin metallic strip (patch) ($t << \lambda_o$, where λ_o is the free-space wavelength) that is on top of a grounded dielectric substrate of thickness h ($h << \lambda_o$, usually $0.003\lambda_o \leq h \leq 0.05\lambda_o$), with relative permittivity and permeability ε_r and μ_r as shown in Figure 2.1 (usually $\mu_r = 1$). The dielectric substrate constants are usually in the range of $2.2 \leq \varepsilon_r \leq 12$ [5, 7]. The one that are most desirable for good antenna performance are thick substrates whose ε_r value is in the lower end of the range because they provide better efficiency, larger bandwidth, loosely bound field for radiation into space, at the expense of larger element size. Thin substrates with higher dielectric constants are desirable for microwave circuitry because they require tightly bound fields to minimize undesired radiation and coupling, and lead to smaller element size; however, because of their greater losses, they are less efficient and have relatively smaller bandwidth [4].

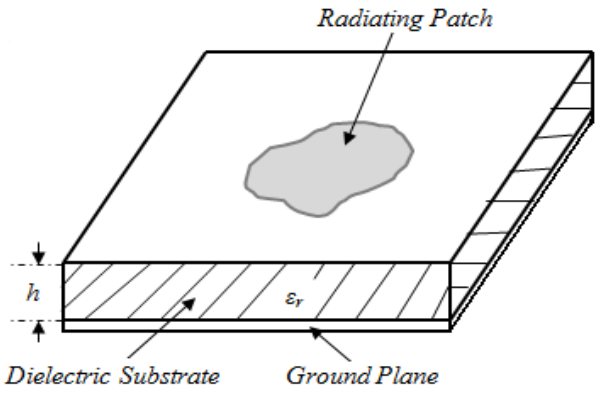

Figure 2.1 *General structure of microstrip antenna [6].*

2.2 Patch Shapes

The radiator should be a material with low ohmic loss and high conductivity at the operating frequency (such as copper or gold). The shape can be an ordinary rectangle, square, ellipse, circle, triangle, ring, and so on. In addition, more complex variations on the basic shapes are frequently used to meet particular design demands, as shown in Figure 2.2. The selection of a particular patch shape depends on some specific requirements such as: polarization, bandwidth, gain, etc. Generally, the antenna's characteristics are defined by the excited operating modes, which depend on the shape and dimensions of the patch, the thickness and dielectric constant of the substrate, as well as the feed arrangement [5].

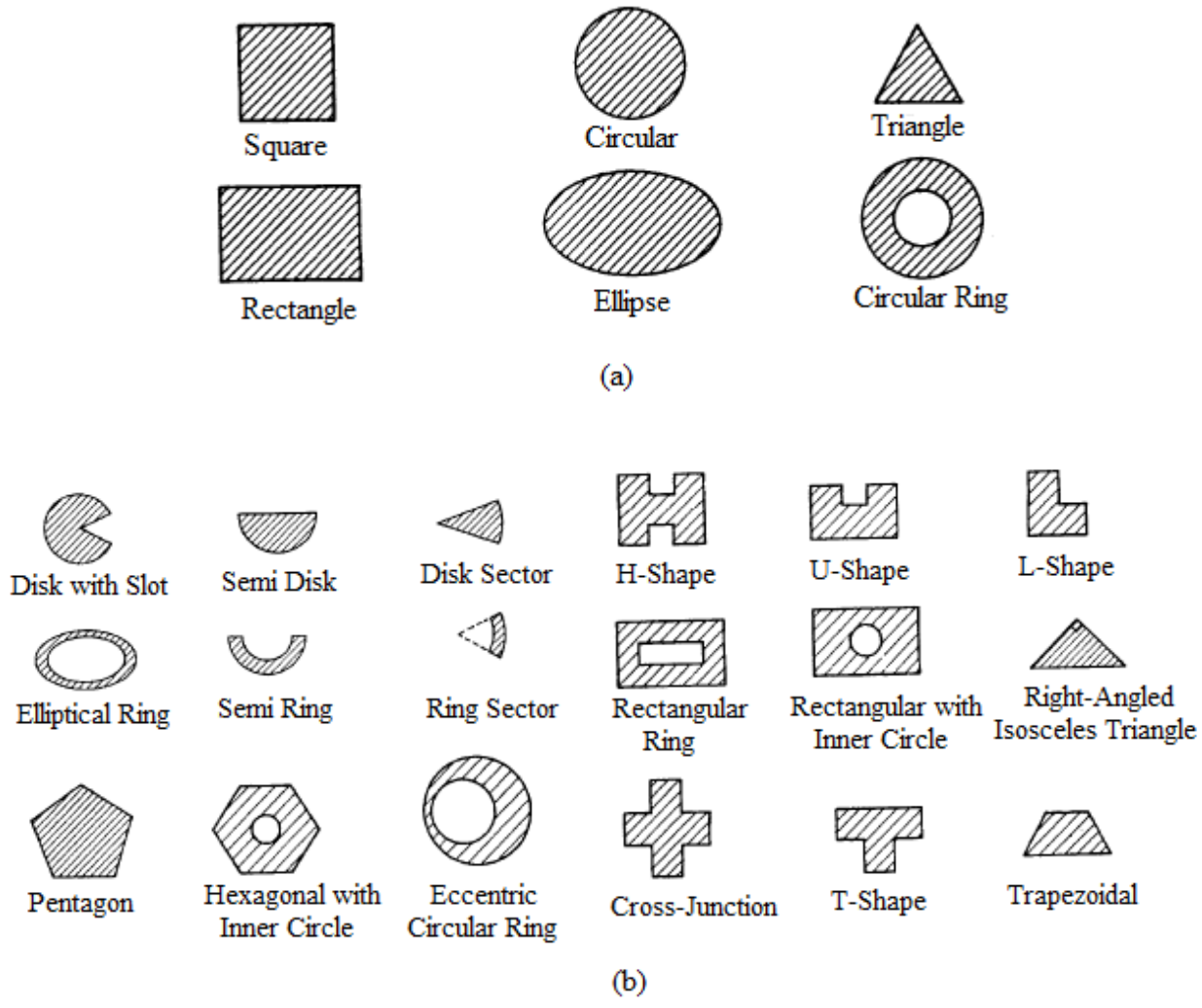

Figure 2.2 *(a) basic microstrip patch antenna shape commonly used in practice; (b) other possible geometries for microstrip patch antennas [4, 5, 6].*

2.3 Advantages and Disadvantages of Microstrip Antennas

MSAs have several advantages compared to conventional microwave antennas. Some of the principal advantages are [4, 6, 7]:

- Light weight, low volume, and thin profile configurations, which can be made conformal;
- Low fabrication cost, readily amenable to mass production;
- Dual-frequency and dual-polarization can be easily made;
- When mounted to a rigid surface they are mechanically robust;
- Can be easily integrated with microwave integrated circuits;
- Feed lines and matching networks can be fabricated simultaneously with the antenna structure;
- Adaptive elements can be made simply adding appropriate placed pin or varactor diodes between the patch and ground plane. Using loaded elements we can vary the antenna's resonant frequency, polarization, impedance, and even its pattern by simply changing bias voltages on the diodes [8].

However, *MSAs* also have disadvantages:

- Narrow bandwidth and associated tolerance problem;
- Lower gain;
- Large ohmic loss in the feed structure of array;
- Complex feed structure is required for high performance arrays;
- Polarization purity is difficult to achieve;
- Poor end-fire radiation, except tapered slot antennas;
- Lower power handling capability;
- Excitation of surface waves.

2.4 Basic Principles of Operation

The metallic patch essentially creates a resonant cavity, where the patch is the top of the cavity, the ground plane is the bottom of the cavity, and the edges of the patch which appears as slots form the sides of the cavity. The edges of the patch act approximately as an open-circuit boundary condition. Hence, the patch acts approximately as a cavity with perfect electric conductor on the top and bottom surfaces, and a perfect magnetic conductor on the sides. This point of view is very useful in analyzing the patch antenna, as well as in understanding its behavior. Inside the patch cavity the electric field is essentially z directed and independent of the z coordinate. Hence, the patch cavity modes are described by a double index *(m, n)* [7].

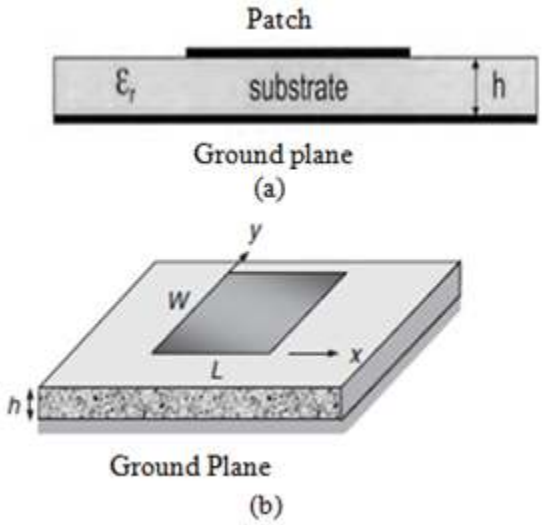

Figure 2.3 *Geometry of microstrip patch antenna: (a) side view showing substrate and ground plane, (b) rectangular microstrip antenna [9].*

Consider the microstrip patch antenna is connected to a microwave source. Energizing the patch will produce a charge distribution on the upper and lower surfaces of the patch, as well as on the surface of the ground plane, as shown in Figure 2.4. The charge distribution is controlled by attractive and repulsive forces. The attractive force is between the corresponding opposite charges on the bottom side of the patch and the ground plane, which tends to maintain the charge concentration on the bottom of the patch. The repulsive force is between like charges on the bottom surface of the patch, which tends to push some charges from the bottom surface, around

its edges, to its top surface. This movement of charges creates corresponding current densities $\boldsymbol{J_b}$ and $\boldsymbol{J_t}$, at the bottom and top surfaces of the patch, as shown in Figure 2.4 [4, 6].

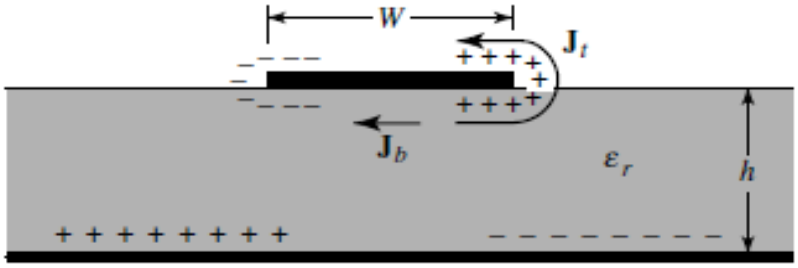

Figure 2.4 *Charge distribution and current density creation on microstrip patch [4, 6].*

For most practical *MSAs*, the ratio h/W is very small. Therefore, the attractive force between the charges dominates and most of the charge concentration and the current flow remain underneath the patch. A small amount of current flows around the edges of the patch to its top surface and is responsible for a weak magnetic field tangential to the edges. Hence, we can make a simple approximation that the tangential magnetic field is zero and one can place magnetic walls all around the periphery of the patch. This assumption has greater validity for thin substrates with high ε_r. Also, since the substrate used is very thin compared to the wavelength ($\boldsymbol{h << \lambda}$) in the dielectric, the field variations along the height can be considered to be constant and the electric field nearly normal to the surface of the patch. Consequently, the patch can be modeled as a cavity with electric walls (because the electric field is near normal to the patch surface) at the top and below and four magnetic walls along the edges of the patch (because the tangential magnetic field is very weak). Therefore, the only possible mode that exists within the cavity is TM_{mn} [6].

For the rectangular patch shown in Figure 2.3(b), the TM_{mn} mode has a normalized electric field that is given by [7, 9]

$$E_z^{mn}(x, y) = \cos\left(\frac{m\pi x}{L}\right)\cos\left(\frac{n\pi y}{W}\right) \qquad 2.1$$

where, L is the patch length and W is the patch width.

Near the patch resonance frequency only one mode is dominant, namely, $m = 1$, $n = 0$. This is the mode associated with the radiation from the patch. The remaining other modes are to represent the interaction between the feed and the patch plus additional energy storage. Therefore, the usual mode of operation for a broadside pattern is the TM_{10} mode, which has no field variation in ***y*** direction [9]. In this mode the patch essentially acts as a wide microstrip line of width W that forms a transmission-line resonator of length L that is approximately one-half wavelength in the dielectric. The width W is usually chosen to be larger than the length L, typically $\boldsymbol{W = 1.5\ L}$ to maximize the bandwidth, since the bandwidth is proportional to the width. However, the width should be kept less than twice the length to avoid the excitation of undesired modes [7, 9].

For the rectangular patch, the dominant TM_{10} mode has an electric field of the form [7, 9]

$$E_z(x, y) = \cos\left(\frac{\pi x}{L}\right) \tag{2.2}$$

The corresponding surface current on the bottom of the metal patch is then ***x*** directed, and is given by [7]

$$J_{sx}(x) = \frac{\pi / L}{j\omega\mu}\sin\left(\frac{\pi x}{L}\right) \tag{2.3}$$

For TM_{10} mode, the electric-field and magnetic-surface-current distributions along the periphery (side wall) and inside the microstrip cavity are illustrated in Figure 2.5. The magnetic currents along the width W are constant and in phase while those along length L vary sinusoidally and are out of phase. The phase reversal along the length is necessary for the antenna to have broadside radiation characteristics. For this reason, the W edge is known as the radiating edge since it contributes predominantly to the radiation. The L edge is known as the non-radiating edge. The current is maximum at the center of the patch, $\boldsymbol{x} = L/2$, while the electric field is maximum at the two radiating edges, $\boldsymbol{x} = 0$ *and* $\boldsymbol{x} = L$, as shown in Figure 2.5(a).

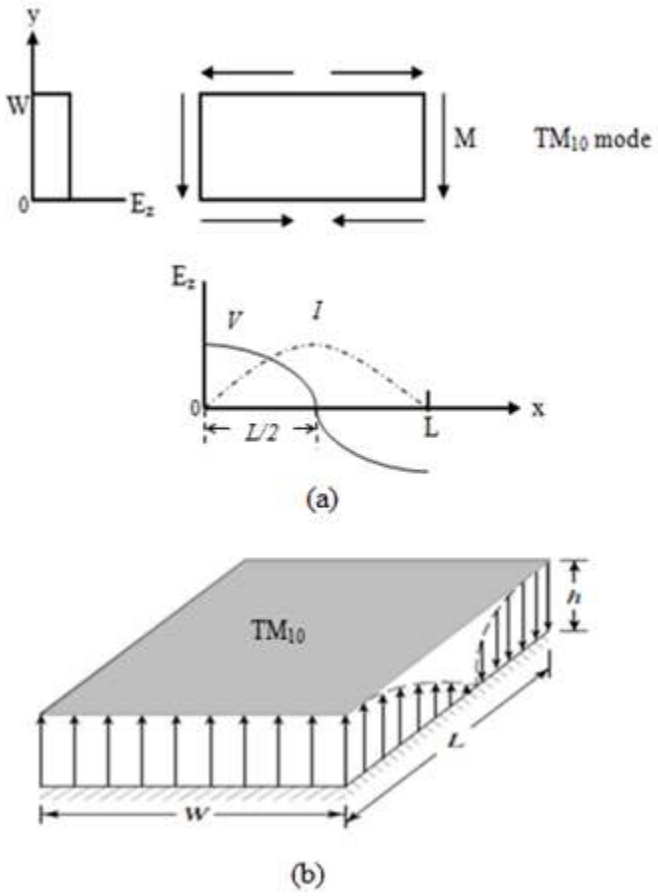

Figure 2.5 *For the dominant TM_{10} mode of a rectangular MSA: (a) electric field and magnetic surface current distributions along the periphery; (b) electric field distribution in the microstrip cavity [4, 6].*

2.5 Antenna Directivity and Gain

The directivity, D, is the measure of the directional properties of an antenna compared to those of an isotropic antenna. The directivity is always greater than 1 since an isotropic radiator is not directional. The directivity is defined as the ratio of the radiation intensity (U) in a given direction from the antenna to the radiation intensity averaged over all directions (U_0). The average radiation intensity is equal to the total power radiated by the antenna divided by 4π. If the direction is not specified, the direction of maximum radiation intensity is implied. Stated more

simply, the directivity of a nonisotropic source is equal to the ratio of its radiation intensity in a given direction over that of an isotropic source [4, 6, 7, 14]. That is,

$$D = \frac{U}{U_0} = \frac{U}{P_{rad}/4\pi} = 4\pi \frac{U}{P_{rad}} \qquad 2.4$$

where U is radiation intensity of a given antenna and U_0 is radiation intensity of an isotropic source.

The expression for approximately calculating the directivity D of the *RMSA* is given by [12]

$$D \cong 0.2W + 6.6 + 10\log\left(\frac{1.6}{\sqrt{\varepsilon_r}}\right) dB \qquad 2.5$$

where W is patch width and ε_r is substrate dielectric constant.

Antenna gain, G, (in a given direction) is defined as the ratio of the intensity, in a given direction, to the radiation intensity that would be obtained if the power accepted by the antenna were radiated isotropically. The radiation intensity corresponding to the isotropically radiated power is equal to the power accepted (input), P_{in}, by the antenna divided by 4π [4, 6, 7, 14].

$$G = 4\pi \frac{U}{P_{in}} \qquad 2.6$$

We can write that the total radiated power (P_{rad}) is related to the total input power (P_{in}) by

$$P_{rad} = e_{cd} P_{in} \qquad 2.7$$

where $e_{cd} = e_c e_d$ is antenna radiation efficiency (i.e., e_c is conduction efficiency and e_d is dielectric efficiency). It is very difficult to compute e_{cd}, but it can be determined experimentally or we can obtain from the simulation output details.

Therefore, Eqn. (*2.6*) becomes

$$G = e_{cd}\left[4\pi\frac{U}{P_{rad}}\right] = e_{cd}\,D \qquad 2.8$$

2.6 Bandwidth Definition

The bandwidth of an antenna is the range of frequencies within which the performance of the antenna, with respect to some characteristic, conforms to a specific standard. Hence, the bandwidth may be calculated by using the frequencies f_u and f_l at the upper and lower edges of the achieved bandwidth [5, 10]

$$BW = \begin{cases} \dfrac{2(f_u - f_l)}{f_u + f_l}\times 100\% & bandwidth\ \left(for\ Narrow\ band\ antenna\right) < 100\% \\ \dfrac{f_u}{f_l}\ :\ 1 & bandwidth\ \left(for\ Wide\ band\ antenna\right) \geq 100\% \end{cases} \qquad 2.9$$

The bandwidth of an antenna can be defined for impedance, radiation pattern and polarization depending on the characteristics selected [5].

- *Impedance* is the basic consideration for all antenna design, which allows most of the energy to be transmitted to an antenna from a feed or a transmission system at a transmitter, and from an antenna to its load at a receiver in a wireless communication system.
- *Radiation pattern* ensures that maximum or minimum energy is radiated in a specific direction.
- *Polarization* of an antenna minimizes possible losses due to polarization mismatch within its operating bandwidth.

In the absence of any stated characteristics preference, the *impedance bandwidth* or *VSWR bandwidth* will be specified for *MSA*. The reason is, it is usually the variation of impedance which limits the standard of the performance rather than the variation of pattern [11]. The bandwidth used in this thesis is targeted at the impedance bandwidth, which is defined below.

2.7 Impedance Bandwidth

In general, microstrip patch antenna is a strongly resonant device. Its input impedance varies greatly with frequency even though the inherent impedance of its feed remains unchanged. If the antenna can be well-matched to its feed across a certain frequency range, that frequency range is defined as its impedance bandwidth. The impedance bandwidth of a *MSA* is determined by its impedance characteristics. A more practical approach is to define it in terms of its input parameters. The return loss (*S* parameter: $|S_{11}|$) or a *VSWR* over a frequency range, is commonly used to define the antenna bandwidth. It is also a meaningful parameter, as it signifies the reflected power not available to the antenna, i.e., the return loss. The *RL* of a *MSA* is normally assumed satisfactory if it is better than -10dB or -15dB. Assuming that the feeding transmission line that connects to the patch is perfectly matched at the resonance frequency; the fractional bandwidth is thus defined as [5]

$$BW = \frac{\Delta f}{f_r} \tag{2.10}$$

where f_r is the impedance resonance frequency of the patch, $\Delta f = f_u - f_l$ is bandwidth, f_u and f_l are the upper and lower frequencies on either side of the resonance frequency.

As the one-port circuit, an antenna is described by a single scattering parameter S_{11} or the reflection coefficient Γ, which gives the reflected signal and quantifies the impedance mismatch between the source and the antenna. Hence, the input *VSWR* and return loss (*RL*) are defined by [12, 15]

$$VSWR = \frac{1 + |\Gamma|}{1 - |\Gamma|} \tag{2.11}$$

$$RL\,(in\ dB) = 20\log\left|\frac{1}{S_{11}}\right| = 20\log\left|\frac{1}{\Gamma}\right| = -20\log|\Gamma| \qquad 2.12$$

The following scale shows the relationship between *VSWR* and return loss [14]:

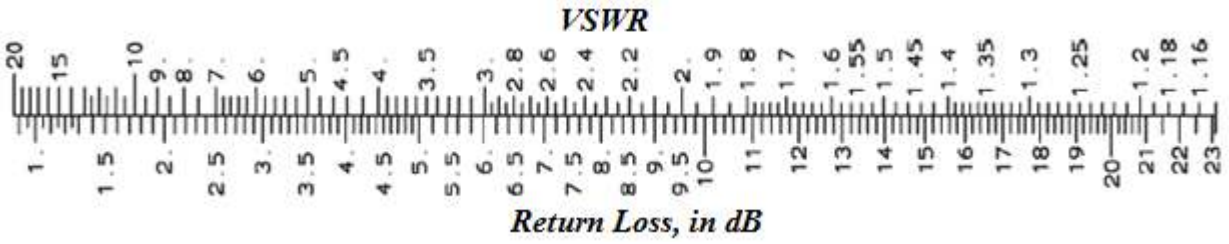

The reflection coefficient, Γ, is a measure of reflected signal at the feed-point of the antenna. It is defined in terms of input impedance Z_{in} of the antenna and the characteristic impedance Z_0 of the feed line as given below [12]

$$\Gamma = \frac{Z_{in} - Z_o}{Z_{in} + Z_o} \qquad 2.13$$

The power reflected back from the antenna is $|\Gamma|^2$ times the power available from the source and the power coupled to the antenna is (1 - $|\Gamma|^2$) times the power available from the source. Therefore, the optimal *VSWR* occurs when $|\Gamma| = 0$ or *VSWR* = 1. This means that all power is transmitted to the antenna and there is no reflection. Practically, $VSWR \leq 2$ (or $|\Gamma| \leq 1/3$) which is translated to a reflection of about 11% of the input power is acceptable for most applications [15]. Figure 2.6 shows the graphical representation of antenna bandwidth definition.

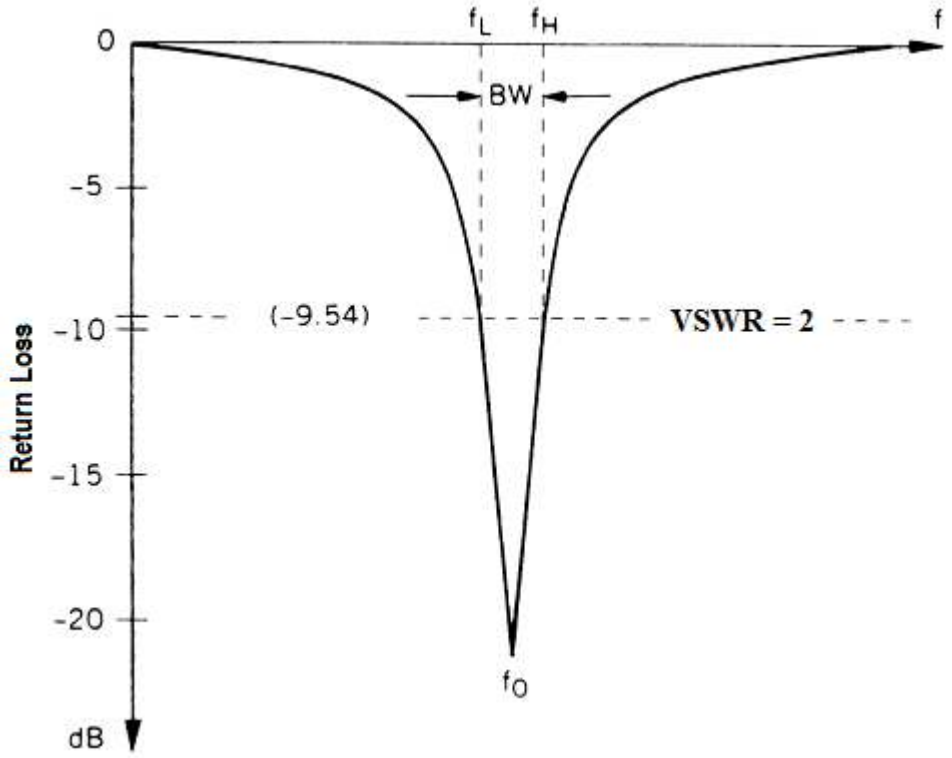

Figure 2.6 *Return loss, S_{11} (in dB) versus frequency [15].*

Then, a more meaningful definition of the fractional bandwidth is over a band of frequencies where the *VSWR* at the input terminals is equal to or less than a desired maximum value, such as *VSWR* = 2 or 1.5 or a return loss, $\boldsymbol{S_{11}}$ of less than −10 dB or −15 dB. Hence, a modified form of Eqn. (*2.10*) that takes into account the impedance matching is [6, 14, 33]

$$BW = \frac{\Delta f}{f_r} = \frac{VSWR - 1}{Q_t \sqrt{VSWR}} \qquad 2.14$$

where Q_t is total quality factor and Eqn. (*2.14*) is valid for $Q_t >> 1$.

If the value of *VSWR* is taken at 2, then Eqn. (*2.14*) will be

$$BW = \frac{\Delta f}{f_r} = \frac{1}{\sqrt{2}\, Q_t} \qquad 2.15$$

An empirical formula by Jackson and Alexopolus for the bandwidth (*VSWR* < *2*) is [6, 22]

$$BW = 3.77\left(\frac{\varepsilon_r - 1}{\varepsilon_r}\right)\left(\frac{h}{\lambda_0}\right)\left(\frac{W}{L}\right) \qquad 2.16$$

In general, bandwidth is proportional to the volume, for instance, for a rectangular microstrip antenna at resonant frequency *BW* can be expressed as [5]

$$\begin{aligned} BW &\propto volume = area \cdot height = length \cdot width \cdot height \\ &\propto \frac{1}{\sqrt{\varepsilon_r}}\frac{1}{\sqrt{\varepsilon_r}}\sqrt{\varepsilon_r} = \frac{1}{\sqrt{\varepsilon_r}} \end{aligned} \qquad 2.17$$

Therefore the bandwidth, *BW*, is inversely proportional to the square root of the dielectric constant, ε_r. Then, lowering the substrate permittivity increases the bandwidth of the patch antenna. However, this has the disadvantage of making the patch larger.

2.8 Quality Factor

For a resonant type of antenna such as the microstrip antenna, it is common to express the physical parameters of interest in terms of the quality factor, or *Q*, of the antenna. It is also useful in determining the *VSWR* bandwidth of the antenna. The quality factor is defined as [9]

$$Q = \omega_r\left(\frac{U_s}{P_{in}}\right) \qquad 2.18$$

where $\omega_r = 2\pi f_r$ is the resonance frequency in radian/s, $\boldsymbol{U_s}$ is the energy stored inside the patch cavity at resonance, and $\boldsymbol{P_{in}}$ is the average power going into the antenna, which is equal to the average power being radiated and dissipated. A microstrip antenna has both dielectric and conductor (ohmic) losses, and possibly surface-wave loss as well. The surface-wave loss depends on the environment surrounding the patch [9].

The total quality factor is related to the component quality factors as [6, 9]

$$\frac{1}{Q_t} = \frac{1}{Q_{sp}} + \frac{1}{Q_{sw}} + \frac{1}{Q_d} + \frac{1}{Q_c} \tag{2.19}$$

where Q_{sp}, Q_{sw}, Q_d, and Q_c denote the space-wave, surface-wave, dielectric and conductor quality factors corresponding to the powers radiated into space, launched into surface-wave, dielectric loss, and dissipated by conductor loss, respectively. The power carried away by the surface wave increases with increase in substrate thickness. However, for thicknesses satisfying [6, 33]

$$\frac{h}{\lambda_0} \leq \frac{0.3}{2\pi\sqrt{\varepsilon_r}} \tag{2.20}$$

the antenna loss associated with the surface wave can be neglected (i.e., $h \leq 1.756\ mm$ in our case, this appears to be the value where the surface wave is about 10% of the space wave and is a reasonable compromise between bandwidth and efficiency in most cases) [33]. The radiation efficiency of the antenna decreases due to the power carried away by the surface waves. Hence, the decrease in efficiency can be used as a criterion in deciding the value of the substrate thickness for the patch.

The variation of Q_t with dielectric constant ε_r, substrate height h and patch width W can be approximated as [6]

$$Q_t \propto \frac{\varepsilon_r}{h},\ similarly\ \ Q_t \propto \frac{1}{W} \tag{2.21}$$

From Eqns. (*2.15*) and (*2.16*), we can approximately obtain the relation between Q_t and dielectric constant ε_r, substrate height h and patch width W as

$$Q_t = \frac{1}{3.77\sqrt{2}} \left(\frac{\varepsilon_r}{\varepsilon_r - 1}\right)\left(\frac{\lambda_0}{h}\right)\left(\frac{L}{W}\right) \tag{2.22}$$

Figure 2.7 shows that *BW* enhancement of conventional *RMSA* is achieved at the values where Q_t is equal to 14.11. This value has been obtained after ***several iterations*** were made to find the values of *W* and *h* (i.e.; *W = 26 mm* and *h = 1.95 mm*). The patch width, *W* was chosen to be ***1.5xL*** in order to get better *BW* and to avoid the excitation unwanted mode, as well. In addition, the substrate height, *h* was carefully chosen considering the value of *h* obtained from Eqn. (*2.20*) and from the values of *h* in the range of $0.003\lambda_o \leq h \leq 0.05\lambda_o$ without affecting the overall antenna radiation efficiency.

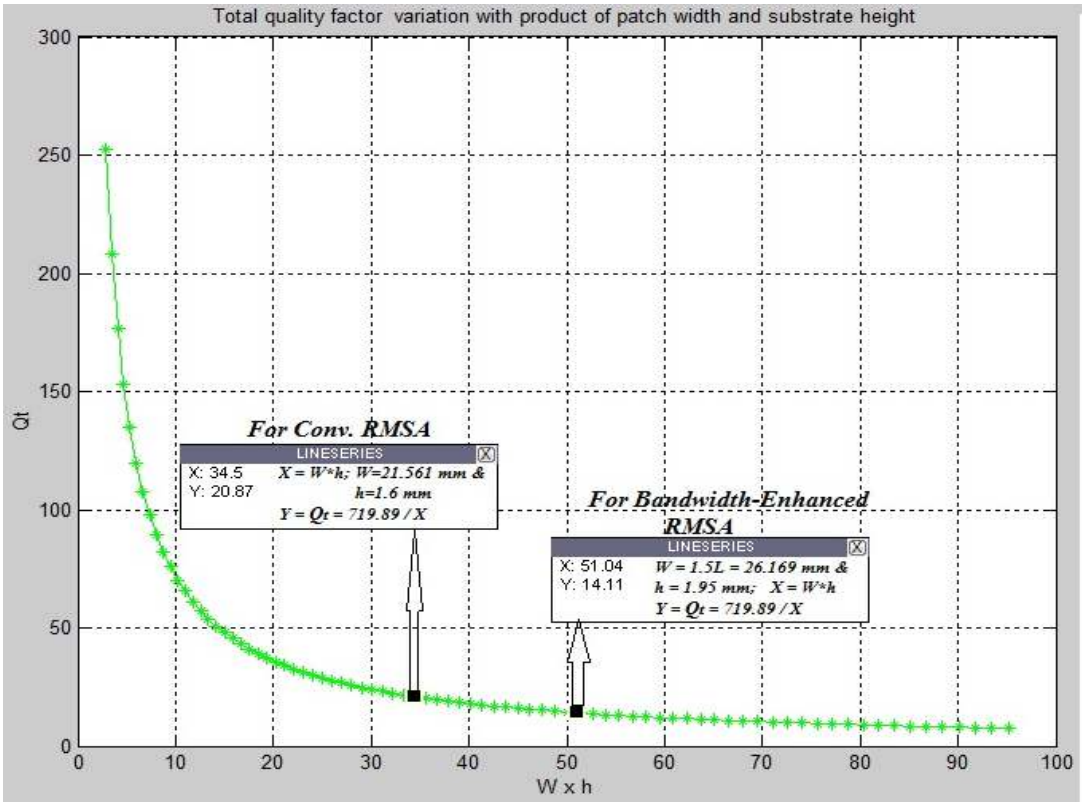

Figure 2.7 *The variation of Q_t of the antenna as a function of W x h for ε_r is 2.2.*

2.9 Method of Analysis

The *MSA* generally has a two-dimensional radiating patch on a thin dielectric substrate and therefore may be categorized as a two-dimensional planar component for analysis purposes. The analysis methods for *MSAs* can be broadly divided into two groups [12].

2.9.1 Analysis Method Based on Magnetic Current Distribution

In this group, the methods are based on equivalent magnetic current distribution around the patch edges (slots) of the antenna. There are three popular analytical techniques, such as:

- *Transmission Line Model;*
- *Cavity Model;*
- *Multiport Network Model* (*MNM*).

These methods offer both simplicity and physical insight. The radiation from the *MSA* is calculated from the equivalent magnetic current distribution around the periphery of the radiating patch, which is obtained from the corresponding voltage distribution. Thus, the *MSA* analysis problem reduces to that of finding the edge voltage distribution for a given excitation and for a specified mode.

2.9.2 Analysis Method Based on Electric Current Distribution

In this second group, the methods are based on the electric current distribution on the patch conductor and the ground plane. Some of the numerical methods for analyzing *MSAs* include:

- *Method of Moments (MoM);*
- *Finite-Element Method (FEM);*
- *Spectral Domain Technique (STD);*
- *Finite-Difference Time Domain (FDTD) Method.*

These techniques give results for any arbitrarily shaped antenna with good accuracy, but they are time-consuming. These methods can be used to plot current distributions on patches but otherwise provide little of the physical insight required for antenna design.

2.10 Bandwidth Enhancement Techniques

Despite a number of useful properties, a narrow bandwidth is a major disadvantage of *MSAs* in practical applications. For present-day wireless communication systems, the required operating bandwidths for antennas are about 7.6% for a *GSM*; 890–960 MHz, 9.5% for a *DCS*; 1710–1880 MHz, 7.5% for a *PCS*; 1850–1990 MHz, and 12.2% for a *UMTS*; 1920–2170 MHz, and so on [13]. To meet these bandwidth requirements, many bandwidth-enhancement or broadband techniques for *MSAs* have been carried out for many years.

A variety of bandwidth enhancement techniques have been developed using the three major approaches categorized under Table 1. It is known that the factors affecting the bandwidth of a microstrip patch antenna are primarily the shape of the radiator, the feeding system, the substrate and the arrangements of radiating and parasitic elements [5].

Table 1 *Broadband techniques for MSAs.*

Approach	*Techniques*
Lower the quality factor, Q	▪ *Select the radiator shape* ▪ *Thicken the substrate* ▪ *Lower the dielectric constant* ▪ *Increase the losses*
Use impedance matching	▪ *Insert a matching network* ▪ *Add tuning elements* ▪ *Use slotting and notching patches*
Introduce multiple resonances	▪ *Use parasitic (stacked or co-planar) elements* ▪ *Use slotting patches, insert impedance networks* ▪ *Use an aperture, proximity coupling*

CHAPTER 3

Coplanar Waveguide Antenna

3.1 The Basics of Coplanar Waveguide

Coplanar waveguide was originally proposed by C. P. Wen from *RCA* Laboratory in 1969. The term *coplanar lines* is used for those transmission line where all the conductors are in the same plane; namely, on the top surface of the dielectric substrate. The original design assumed the adjacent ground strip widths and dielectric thickness were infinite as shown in Figure 3.1. Over the years, many inventors modified the design to achieve superior attenuation and dispersion characteristics for meeting specific applications.

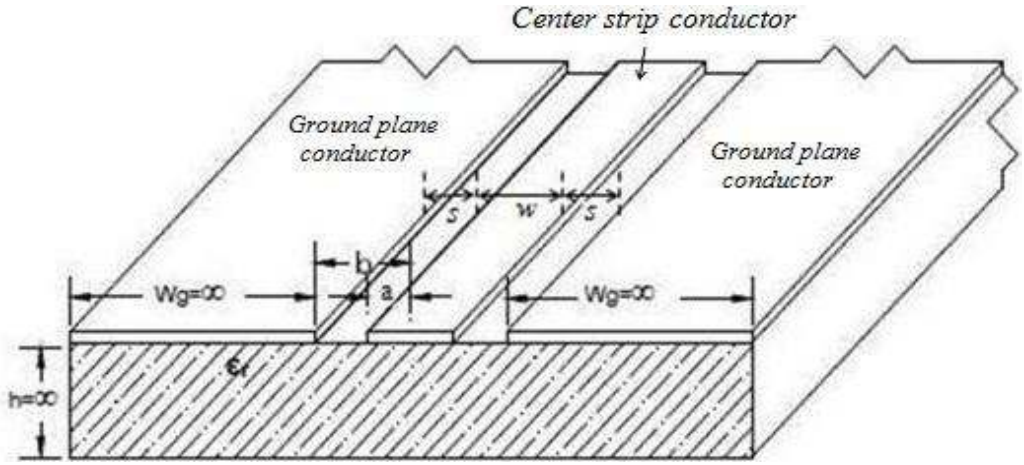

Figure 3.1 *A perspective view of a conventional CPW showing center conductor width w (w=2a), and slot (gap) width s (s=b-a), with infinite ground plane widths (Wg=∞) and infinite dielectric material thickness (h=∞).*

A conventional *CPW* on a dielectric substrate consists of a center strip conductor with semi-infinite ground planes on either side is shown in Figure 3.2. This structure supports a *quasi-TEM* mode of propagation [23, 24].

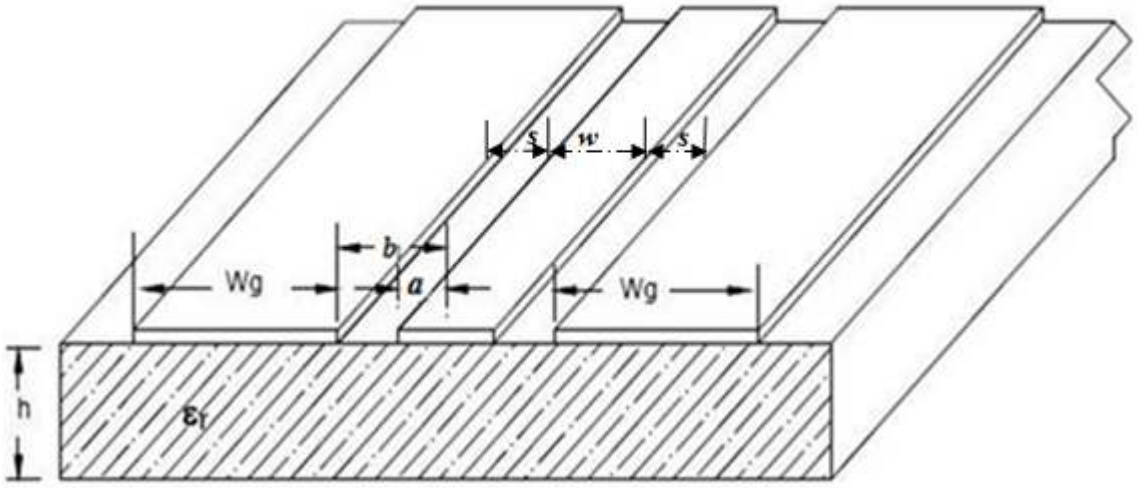

Figure 3.2 *A perspective view of symmetrical CPW showing the finite width of ground plane conductor.*

Since the *CPW* has the central strip and the ground planes both on top of the dielectric carrier material, it forms a real planar waveguide. Because, in principle, it is a three-conductor line, it can carry two fundamental modes: (a) the so-called "*even mode*" which has equal potentials of the ground planes, and (b) the so-called "*odd mode*" which has ground potentials of different signs but equal magnitude.

Figure 3.3 shows the electric and the magnetic field distribution of (a) the even mode (*coplanar waveguide mode*) and (b) the odd mode (*slotline mode*). The even mode is a *quasi-TEM* mode with even symmetry with respect to the symmetry plane, its dispersion is very low [24], and it is normally used for application in circuit design. The electric field lines begin (or end) at the center conductor and they end (or begin) on the two surrounding ground planes. The magnetic field lines enclose the center conductor. If current is transported on the center conductor (e.g., with direction into the paper plane as shown in Figure 3.3(a)), the current densities in the ground planes have the opposite direction. Because of the low dispersion of the fundamental "even mode" very broadband applications are possible, making this mode propagation applicable in microwave integrated circuits.

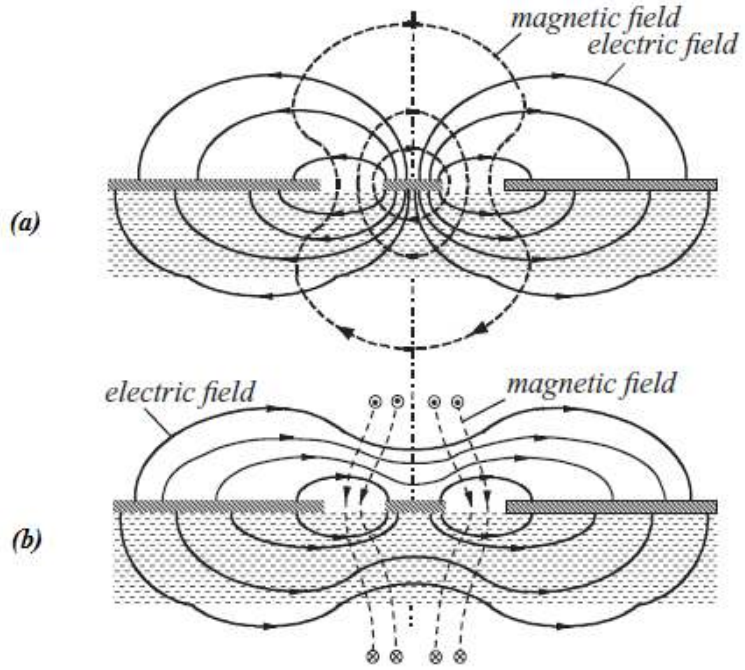

Figure 3.3 *Electric and magnetic field distribution of (a) the even mode and (b) the odd mode on a coplanar waveguide [24].*

The electric field lines of the odd mode start on one ground plane and end on the other ground plane as shown in Figure 3.3(b), which means that the potentials of the two ground planes have opposite signs. Not all of the electric field lines touch the center conductor. In the case of infinitely wide ground planes the odd mode, like a slot-line mode, is a hybrid mode and has magnetic field components in longitudinal direction and its dispersion can be considered large. If the ground plane width is finite, the magnetic field lines may be closed in the cross section enclosing the ground planes [24].

3.2 CPW Advantages and Disadvantages

The *CPW* offers several advantages over conventional microstrip line:

- It simplifies fabrication, facilitates easy shunt as well as series surface mounting of active and passive devices.
- The characteristic impedance Z_0 is determined by the ratio of $w/(w+2s)$ as shown in Eqns. (*3.4*) and (*3.10*), so size reduction is possible without limit because the design

of a *CPW* line with a particular Z_0 is non-unique, i.e., an infinite range of w and s values will result in a specific Z_0 requirement. However, a similar situation does not, unfortunately, exist with microstrip. Because the characteristic impedance Z_0 is very largely determined by the ratio of strip width (usually denoted W) to height h and the substrate permittivity ε_r. This results in a unique value of W for a required Z_0 as h is nearly always fixed by an earlier design decision.

- Immediate access to adjacent power planes provide shorter power delivery path (i.e. lower inductance) to boost active devices performance.
- Bottom reference plane provides structural strength.
- In some cases, *CPW* gives lower conductor losses and dispersion.
- Adjacent strips provide excellent isolations to minimize crosstalk on the same metallization layer.
- Coplanar circuits can be designed smaller in size than microstrip-based integrated circuits because additional ground planes on top of the substrate can reduce the coupling between adjacent lines. In fact, space reduction in the order of 30–50% [24] is possible if coplanar circuits are used instead of microstrip-based circuits.

Likewise, there are also disadvantages of *CPW* circuits where some are listed below.

- Parallel plate configuration produces zero cutoff frequency modes.
- *CPW* without conducting plane has lower thermal dissipation and lower structural strength.
- In general, *CPW* experience higher losses compared to microstrip.
- High frequency losses due to over-moding are more common on *CPW* than microstrip.
- The two fundamental modes can propagate on the line with zero cutoff frequency if the two ground planes are not held at the same potential.
- *CPW* side strips generate both odd and even modes current that can cause serious mode coupling.

3.3 Method of Analysis

Coplanar lines have been studied using quasi-static approximation methods or full-wave methods. While full-wave methods are at the same time the most accurate tools for obtaining the *TL* characteristics and the most analytically extensive, quasi-static methods are quite simple but do not treat the dispersive nature of a generic *TL*. Consequently, the approximation of the *QSM* becomes worse as the *TL* becomes dispersive. It is known that the error in the *QSM* increases if the *TL* does not support a "*TEM*" or "*quasi-TEM*" mode. With certain assumption and approximation *CPW* (the approximation is very good until 20 GHz) can support a "*quasi-TEM*" mode, so that the *CPW* transmission line characteristics can be studied by employing two simple *QSMs*, i.e., the "*conformal transformations (mapping)*" and "*finite differences*". However, in this thesis we used the "*conformal transformations*" method since it is the simplest and most often used *QSM* [29].

3.3.1 CPW Analysis Using Conformal Transformations Method

Figure 3.4 shows the *CPW* as it is used in most applications. In principle, it is a planar three-strip line [23, 24]. For a true *TEM-mode* propagation on a waveguide, a homogeneous medium is needed in the cross section of the line. In the case of the *CPW*, the field carrying space of the line has a piecewise homogeneous medium only. This, as is well known, leads to different phase velocities of possible waves in the different media. Because of the boundary conditions in the plane between the media, only one mode with a common phase velocity in all media can propagate along the line, so that a hybrid mode is built up which has not only transversal field components, but also longitudinal electric and magnetic field components [24]. In the case of the *fundamental coplanar mode*, these field components are small compared to the transversal components, especially at low frequencies. But with increasing frequency the influence of these *longitudinal components* becomes larger. This means that the wave propagation along the line can no longer be described using frequency-independent characteristic parameters (impedance, phase velocity). This frequency dependence of the line parameters, which is called the *dispersion* of the line parameters, is strongly dependent on the field distribution and the geometrical parameters of the considered line [24].

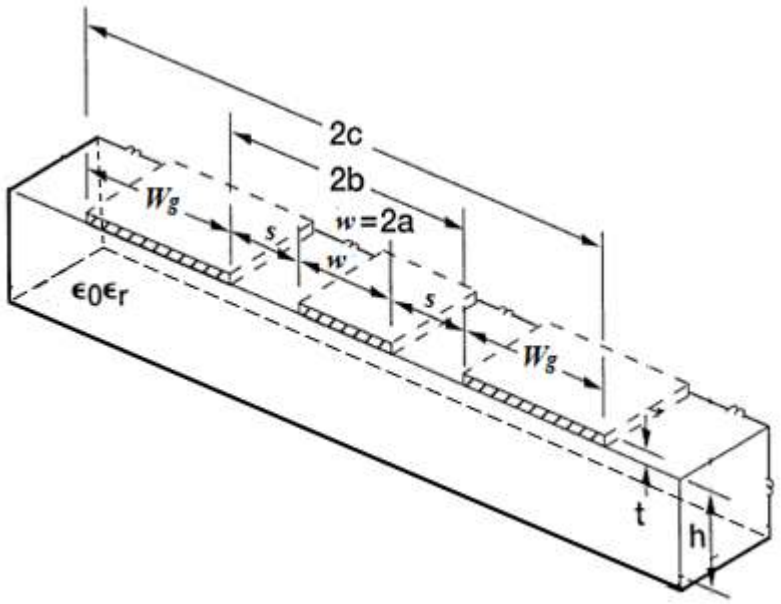

Figure 3.4 *CPW Schematic with finite width and finite dielectric thickness [23].*

In brief, the basic approach used in the conformal transformation method is to assume that the dielectric substrate has perfect conductivity and relative permittivity, respectively. Hence the structure is considered to be lossless. Further the dielectric substrate materials are considered to be isotropic. In addition, the conductor (metallic) thickness ***t*** is assumed to be zero, as shown in Figure 3.5(a), and magnetic walls are present along all the dielectric boundaries including the *CPW* slots. The *CPW* is then divided into several partial regions that resemble a parallel plate capacitor and the electric field is assumed to exist only in that partial region, then the capacitance of each partial region is determined separately [16, 23].

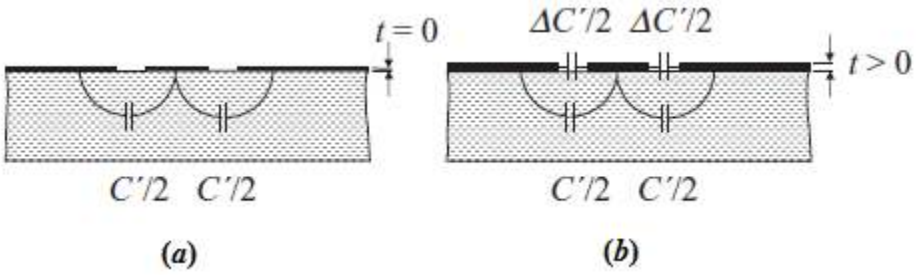

Figure 3.5 *The influence of the metallization thickness on the line parameters of the CPW [24].*

Hence, the approximate value of effective permittivity ε_{reff} and characteristics impedance Z_0 will be determined using conformal mapping method [23]. In this manner the total capacitance of the coplanar waveguide C_{CPW} is then the sum of the partial capacitances C_1 and C_{air} [23, 24, 25, 26]

$$C_{CPW} = C_1 + C_{air} \tag{3.1}$$

where C_1 is the partial capacitance of the *CPW* with the dielectric layer and C_{air} is the partial capacitance of *CPW* in the absence of the dielectric layer.

The effective dielectric constant ε_{reff} has also the following relation:

$$\varepsilon_{reff} = \frac{C_{CPW}}{C_{air}} \tag{3.2}$$

The expressions for the partial capacitances C_1 and C_{air} of the *CPW* will be given by [23, 24, 25]

$$C_1 = 2\varepsilon_0(\varepsilon_r - 1)\frac{K(k_1)}{K(k_1')}, \quad and \quad C_{air} = 4\varepsilon_0 \frac{K(k_0)}{K(k_0')} \tag{3.3}$$

where ε_0 is free space permittivity, i.e.; $\varepsilon_0 = 8.854 \times 10^{-12}$ *F/m.*

The modulus (i.e.; k and k_0) and complementary modulus (k' and k_0') of the complete elliptical integrals $K(k_1)$, $K'(k_1) = K(k_1')$, $K(k_0)$, $K'(k_0) = K(k_0')$ are given by

$$k_1 = \frac{\sinh(\pi w/4h)}{\sinh\{[\pi(w+2s)]/4h\}}, \quad and \quad k_1' = \sqrt{1-k_1^2}$$

$$k_0 = \frac{w}{w+2s}, \quad and \quad k_0' = \sqrt{1-k_0^2} \tag{3.4}$$

In general the function *K(k)* is called the complete elliptical integral of first kind, and $K'(k_1) = K(k_1')$ is the complete elliptical integral of the second kind. They are expressed by

$$K(k) = \int_0^1 \frac{d\xi}{\sqrt{(1-\xi^2)(1-k^2\xi^2)}}$$

and

3.5

$$K'(k) = K(k') = \int_0^1 \frac{d\xi}{(1-\xi^2)(1-\xi^2+k^2\xi^2)}$$

where ξ is the real part of the complex modulus (or arguments).

Substituting Eqn. (*3.3*) in Eqn. (*3.1*), we obtained

$$C_{CPW} = C_1 + C_{air} = 2\varepsilon_0(\varepsilon_r - 1)\frac{K(k_1)}{K(k_1')} + 4\varepsilon_0\frac{K(k_0)}{K(k_0')} \quad 3.6$$

which yields,

$$\varepsilon_{reff} = \frac{C_{CPW}}{C_{air}} = 1 + \frac{(\varepsilon_r - 1)}{2}\frac{K(k_1)}{K(k_1')}\frac{K(k_0')}{K(k_0)} \quad 3.7$$

In a well-designed case of a coplanar waveguide, the fields of the even mode are kept close to the gaps and this situation does not change much with frequency, especially not if the slot width ***s*** is small. If the height of the dielectric carrier material is large or if there is no air region under the substrate, then the effective dielectric constant of the even mode as a first approximation is given by [24]

$$\varepsilon_{reff} = \frac{(\varepsilon_r + 1)}{2} \quad 3.8$$

Further, the phase velocity v_{ph} and characteristic impedance Z_0 are defined as

$$v_{ph} = \frac{c}{\sqrt{\varepsilon_{reff}}}$$
$$and$$
$$Z_0 = \frac{1}{C_{CPW} v_{ph}} = \frac{1}{(\varepsilon_{reff} C_{air})(c/\sqrt{\varepsilon_{reff}})} = \frac{1}{c C_{air}\sqrt{\varepsilon_{reff}}} \quad 3.9$$

where c is the velocity of light in free space (i.e., $c = 3x10^8$ *m/s*).

Therefore, the characteristic impedance Z_0 becomes

$$Z_0 = \frac{1}{c C_{air}\sqrt{\varepsilon_{reff}}} = \frac{30\pi}{\sqrt{\varepsilon_{reff}}} \frac{K(k_0')}{K(k_0)} \quad 3.10$$

Note that, the general expression for the ratio of $K(k)/K(k')$ is given by the following expression

$$\frac{K(k)}{K(k')} = \begin{cases} \left[\frac{1}{\pi}\ln\left(2\frac{1+\sqrt{k}}{1-\sqrt{k}}\right)\right]^{-1} & for\ 0 \le k \le 0.707 \\ \frac{1}{\pi}\ln\left(2\frac{1+\sqrt{k}}{1-\sqrt{k}}\right) & for\ \ 0.707 \le k \le 1 \end{cases} \quad 3.11$$

Note that, Hoffmann, in his handbook, argues that when the ground-plane width W_g fulfills the condition $W_g \ge 0.5(w+2s)$, the effect of the ground width on the characteristic impedances of the even and the odd mode can be neglected [24, 28]. However, the effective dielectric constant of the odd mode strongly decreases with increased values of W_g because in the case of a large ground-plane width, the electric field concentration in air is much higher than in the case of small ground plane width. However, the effective dielectric constant of the even mode, which is of

more interest to the circuit designer, is less affected by the width of the ground planes because the electromagnetic field is concentrated in the area around the gaps [24].

3.4 CPW Patch Antennas

A radiating element is constructed from a *conventional CPW structure* by widening the center strip conductor to form a *rectangular* or *square patch*. This patch produces a single-lobe, linearly polarized pattern directed normal to the plane of the conductors. The advantage gained over conventional microstrip patch antenna is lower cross polarized radiation from the feed [23]. The feed system in these antennas is directly coupled, electromagnetically coupled, or aperture coupled to the patch.

CHAPTER 4

Antenna Design

In this thesis I have chosen rectangular-patch shape for both microstrip and coplanar waveguide antennas design. Rectangular patch shape is selected because it is easy for analysis and it is commonly used configuration.

4.1 Feeding Technique

The feed element (or port) is to transfer *RF* or microwave energy efficiently from the transmission system to the antenna radiator. Selection of the feeding technique is governed by number of factors [6]. The most important consideration is the efficient transfer of power between the radiating structure and feed structure, that is, ***impedance matching*** between the two. In general, the design of the feeding structure directly governs the impedance matching, operating modes, spurious radiation, surface waves and the geometry of the antenna. Therefore, the feeding structure plays a vital role in widening the impedance bandwidth and enhances radiation performance [5].

In EMPIRE simulation software, there are several feeding techniques (ports) available to transmit electromagnetic energy to the radiating structure. Such as: ***coax*** or ***probe***, ***microstrip line*** (***MSL***), ***stripline***, ***waveguide*** (***WG***), ***coplanar waveguide*** (***CPW***), and ***lumped***.

Therefore, in this thesis, coupling electromagnetic energy from the source to the radiating patch was fed by using ***lumped port***. Because, at *RF* and *low microwave frequencies*, lumped-elements can be used in the circuit design if the length of its element is very small in comparison to the wavelength and they have the advantages of *small size* and *wider bandwidth*, *lower cost* and they have *lower quality **(Q)** factor*. Previously lumped element was limited to 10 GHz; however, with the advent of new *photolithographic techniques*, the fabrication of lumped elements can now be extended to 60 GHz and beyond. Therefore, lumped-elements can be used for feeding *RF* power

to the patch in both *RMSA* and *CPW-RPA* configurations since its impedance value can be easily tuned to the desired values [15, 16, 17].

In general, a lumped port is [18]:

- A general purpose port which is commonly used when a compact port is required;
- Cannot be placed on the boundary – must be placed inside the boundary;
- It consists of a current source with a parallel load (*with default impedance*: 50 Ω) as shown in Figure 4.1(b);
- Incident and reflected waves are separated using the reference impedance.

A *lumped-element* in microwave circuits is defined as a *passive component* whose size across any dimension is much smaller than the operating wavelength so that there is no appreciable phase shift between the input and output terminals. Generally, keeping the maximum dimension less than $\lambda/20$ is a good approximation where λ is guide (dielectric) wavelength.

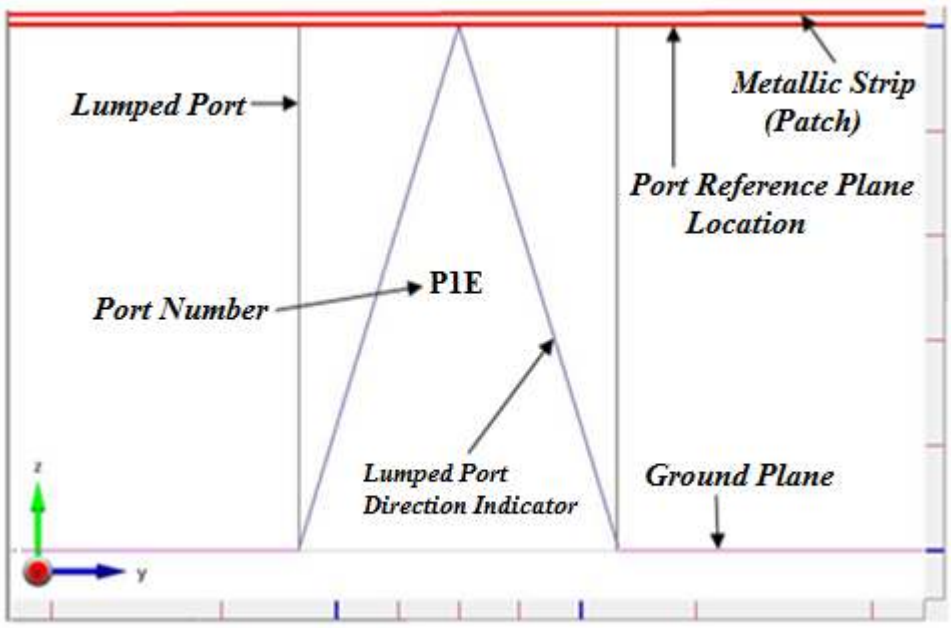

(a)

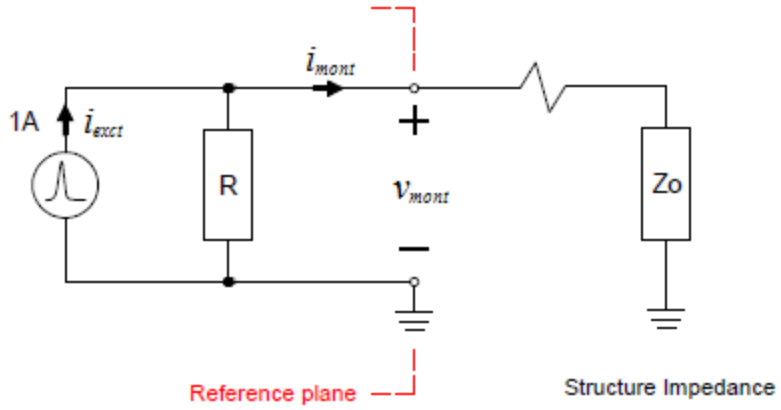

(b)

where

i_{excit} : current excitation source (user definable waveform with 1A amplitude)
R: user defined port reference impedance
Z_o: input impedance of the patch (structural impedance)
i_{moni} : current monitor results generated by Empire (A)
v_{moni} : voltage monitor results generated by Empire (V)

Figure 4.1 *RF coupling system (a) lumped port terminating a metallic strip (patch), and (b) lumped port schematic diagram[18].*

4.2 Rectangular Microstrip Antenna

The rectangular shape is one of the simplest and widely used *MSA* configurations in practice because of its simple shape and attractive characteristics. The basic antenna element is strip conductor (patch) of dimension L x W, as shown in Figure 4.2, on a dielectric substrate of dielectric constant ε_r and thickness h backed by the ground plane. The coordinate axis is selected such that the length L is along the ***x*** direction and width W is along the ***y*** direction.

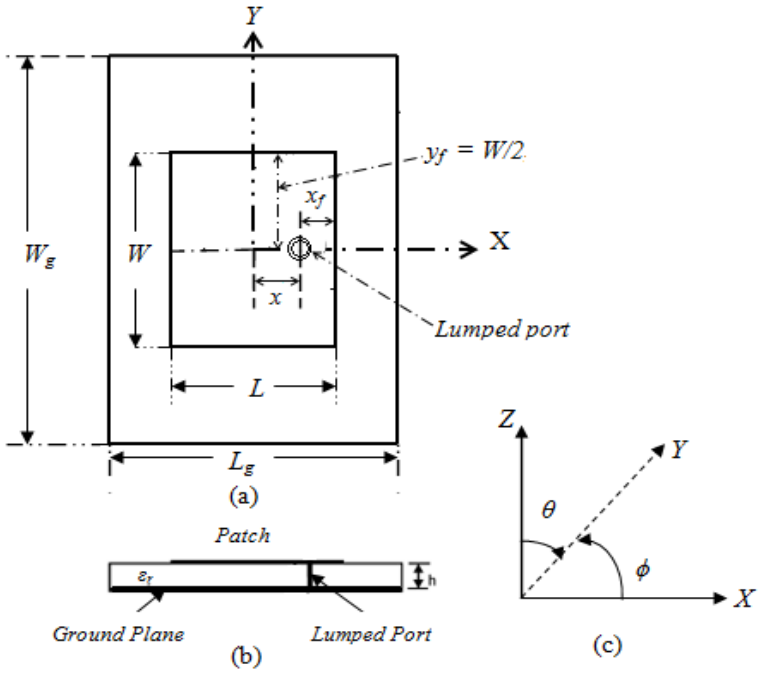

Figure 4.2 *A RMSA with lumped port (a) top view; (b) side view; (c) coordinate system [12].*

4.2.1 Transmission Line Modeling

The objectives of antenna analysis are *to predict* the radiation characteristics such as radiation patterns, gain, and polarization as well as input impedance, bandwidth, mutual coupling, antenna efficiency, and so on. Modeling *RMSA* with a transmission-line for analytical approach is the simplest of all and it gives good physical insight but it is less accurate. It represents the antenna by two slots of width *W* and height *h* separated by a transmission line of length *L*, as shown in Figure 4.3(c).

A *RMSA* operating at TM_{10} mode can be visualized as a transmission-line, because the field is uniform along the width and varies sinusoidally along the length. The fringing fields along the edges and radiation from the slots are modeled by their equivalent susceptance *B* and conductance *G* separated by the length *L* of the patch; respectively, as shown in Figure 4.3(d). Due to the dimensions of the patch are finite (i.e., in length and width) the fields at the edges of the patch undergo fringing. The fringing fields act to extend the effective length of the patch.

Thus, the length of a half-wave patch is slightly less than a half wavelength in the dielectric material.

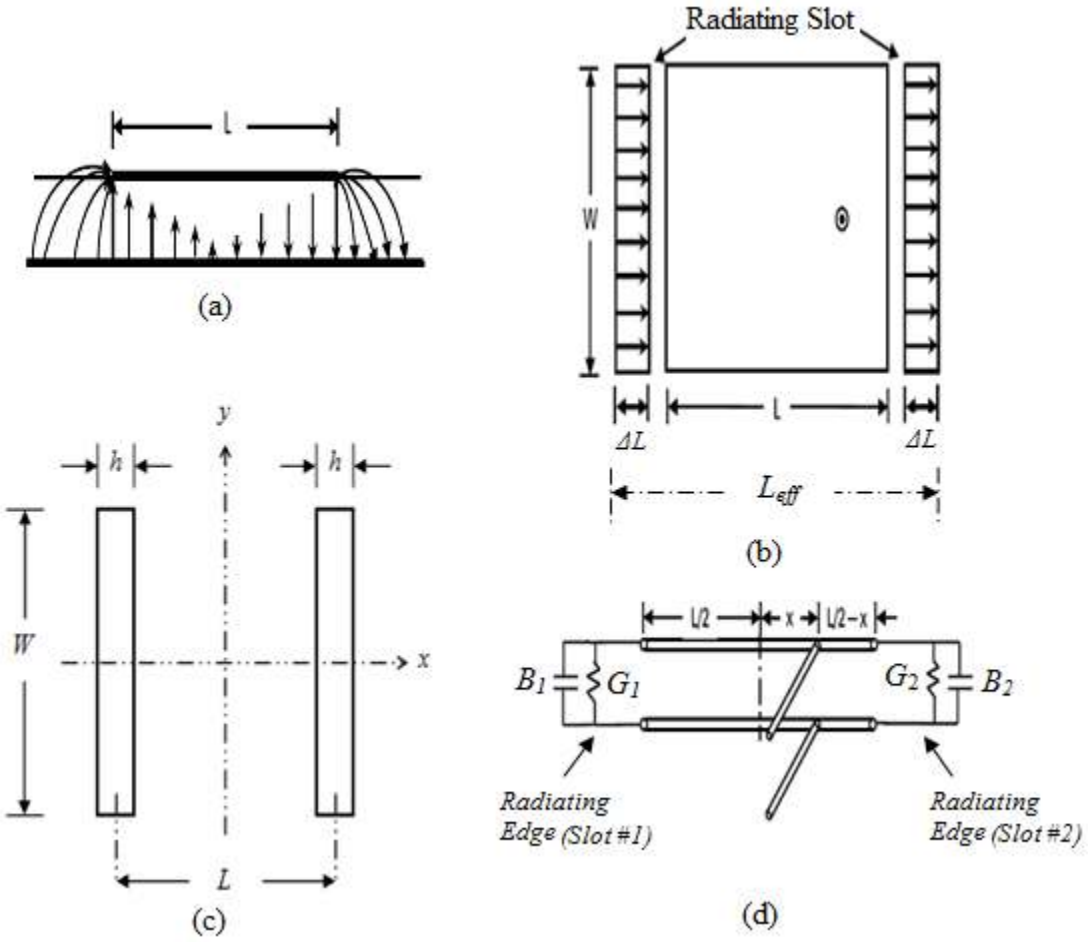

Figure 4.3 *For the fundamental TM_{10} mode of RMSA: (a) electric field distribution (**fringing effect**); (b) two radiating slots (c) two-slot model of a rectangular patch antenna; and (d) equivalent transmission-line model [12].*

4.2.2 Fringing Effect

Figure 4.3(a) shows the presence of field lines in the air at the edges of the patch, which is called fringing field. This is a nonhomogeneous line of two dielectrics; typically the substrate and the air. The amount of fringing is a function of the width of the patch *W* and the height *h* of the substrate. As can be seen, most of the field lines reside in the substrate and parts of some lines

exist in air. If all the fields existed between the patch and the ground plane, the dielectric constant would be that of the substrate. Instead it is somewhat less than that of a substrate. Therefore, an effective dielectric constant ε_{reff} is introduced to account for fringing and the wave propagation in the air. That is, the expression for ε_{reff} is given by [4, 6, 17]

$$\varepsilon_{reff} = \frac{\varepsilon_r + 1}{2} + \frac{\varepsilon_r - 1}{2}\left[1 + 12\frac{h}{W}\right]^{-1/2}, \qquad (W/h > 1) \tag{4.1}$$

For a rectangular microstrip patch antenna, the resonance frequency, f_r for any TM_{mn} mode is given by [12]

$$f_r = \frac{c}{2\sqrt{\varepsilon_r}}\left[\left(\frac{m}{L}\right)^2 + \left(\frac{n}{W}\right)^2\right]^{1/2} \tag{4.2}$$

where c is free-space speed of light, m and n are modes along the L and W, respectively.

For the dominant TM_{10} mode, the resonant frequency of the microstrip antenna is a function of its length. Now Eqn. (4.*2*) reduces to

$$f_r = \frac{c}{2L\sqrt{\varepsilon_r}} \tag{4.3}$$

In practice, the fields are not confined to the patch. A fraction of the fields lie outside the physical dimensions of the patch due to fringing effect. Hence, Eqn. (*4.3*) must be modified to include the edge effect and we obtain

$$f_r = \frac{c}{2L_{eff}\sqrt{\varepsilon_{reff}}} \tag{4.4}$$

where L_{eff} is effective length and it is shown in Figure 4.3(b).

4.2.3 Patch Width and Length

Patch width has a minor effect on the resonant frequency and radiation of the antenna; but it affects the input resistance and bandwidth to a larger extent. That is, a larger patch width increases the power radiated with a decrease in resonant resistance, increase in bandwidth, and an increase in radiation efficiency. With proper excitation we can choose a patch width greater than the patch length without exciting undesired modes. The disadvantage of larger width *W* is the generation of grating lobes (multiple main beams) in antenna arrays, and increasing patch size which is not preferred. The patch width should be selected to obtain good radiation efficiency and it is suggested that $1 < W/L < 2$ [6].

For an efficient radiator, a practical width *W* that leads to good radiation efficiencies is given by [4, 12]

$$W = \frac{c}{2 f_r} \sqrt{\frac{2}{\varepsilon_r + 1}} \tag{4.5}$$

However, the patch length determines the resonance frequency and it is a critical parameter in the design of microstrip antenna [6]. The lowest-order mode, TM_{10}, resonates when the effective length L_{eff} across the patch is a half-wavelength *(λ/2)*. Hence, from Eqn. (4.*4*) we obtain

$$L_{eff} = \frac{c}{2 f_r \sqrt{\varepsilon_{reff}}} = \frac{\lambda_o}{2 \sqrt{\varepsilon_{reff}}} = \frac{\lambda}{2} \tag{4.6}$$

Eqn. (*4.6*) implies that the fundamental TM_{10} mode field varies one *λ/2* cycle along the length, and there is no variation along the width of the patch. Therefore, in order to operate in this mode, the length *L* of the patch must be slightly less than *λ/2* (i.e., $L < \lambda/2$) where λ is the wavelength in the dielectric medium and is equal to $\lambda = \lambda_o / \sqrt{\varepsilon_{reff}}$, and $\lambda_o = c / f_r$ is free-space wavelength.

It is observed from Figure 4.3(a) and (b) that the vertical components of the electric field (*E-field*) at the two edges along the width are in opposite directions and hence cancel one another in the broadside direction, whereas the horizontal components are in the same direction and hence combine in the broadside direction. Therefore, the edges along the width are termed as radiating edges. The fields due to the sinusoidal distribution along the length cancel in the broadside direction, and hence the edges along the length are known as nonradiating edges. The fringing fields along the width can be modeled as radiating slots as shown in Figure 4.3(b) [12].

Because of the fringing effects, the electrical length of the patch of the microstrip antenna looks greater than its physical dimensions as shown in Figure 4.3(b). That is, the dimension of the patch length on each end is extended by a distance ΔL, which is a function of the effective dielectric constant ε_{reff} and the width-to-height (W/h) ratio. A practical approximate relation for the normalized extension of the length is given by [4, 5, 6, 7, 14]

$$\frac{\Delta L}{h} = 0.412 \frac{\left(\varepsilon_{reff} + 0.3\right)\left(\frac{W}{h} + 0.264\right)}{\left(\varepsilon_{reff} - 0.258\right)\left(\frac{W}{h} + 0.8\right)} \tag{4.7}$$

From Figure 4.3(b), the effective length of the patch is

$$L_{eff} = L + 2\Delta L \tag{4.8}$$

The actual length of the patch can now be determined using Eqns. (*4.6*) and (*4.8*)

$$L = \frac{c}{2 f_r \sqrt{\varepsilon_{reff}}} - 2\Delta L \tag{4.9}$$

4.2.4 Ground Plane Dimensions (L_g and W_g)

The transmission line model, cavity model, and multi-network model only consider infinite ground plane. However, in practice, the size of the ground plane is finite. The finite ground plane effect can be taken into account by numerical techniques. However, it should be noted that the simulation time is least when the ground plane is infinite because only the patch is analyzed with its perfect image. For the finite ground plane, on the other hand, both the patch and the ground plane are divided into number of segments and hence the simulation time increases. However, similar results for finite and infinite ground plane can be obtained if the size of the ground plane is greater than the patch dimensions by approximately six times the substrate thickness all around the periphery [12]. Hence, the ground plane dimensions would be given by

$$W_g = 6h + W$$
$$L_g = 6h + L \qquad 4.10$$

4.2.5 Feed Point Location

After determining the patch dimensions L and W for a given f_r, ε_r and h, the next step is to determine the feed point location (x_f, y_f) so as to obtain a good impedance match between the generator impedance (i.e., usually taken to be 50 Ω) and the input impedance of the patch element. Although the feed point can be selected anywhere along the patch width, for linear polarization the patch is usually fed along the centerline $y_f = W/2$. So that TM_{0n} modes (n is odd) will not be excited along with the TM_{10} mode. If the patch is fed at a distance x_f from one of the radiating edges along the patch length or x distance from the center of the patch (i.e., $x = \frac{L}{2} - x_f$) along its length, then the value for x_f or x is given approximately by [6, 14]

$$x_f = \frac{L}{\pi}\cos^{-1}\sqrt{\frac{R_{in}}{R_e}}$$

or

$$x = \frac{L}{\pi}\sin^{-1}\sqrt{\frac{R_{in}}{R_e}} \qquad 4.11$$

where both R_{in} and R_e are defined in Eqns. (4.*12*) and (*4.16*).

4.2.6 Resonant Input Impedance

For the fundamental TM_{10} mode, since there is maximum voltage and minimum current at the edges as shown in Figure 2.5(a), the input impedance of the *RMSA* varies from a zero value at its center to the maximum value at the radiating edges. Hence, feed point location controls the resonant input impedance. When the patch is fed at the edge of the patch (x_f = 0) the input impedance is highest and smallest (essentially zero) when the patch is fed at the center ($x_f = L/2$). Therefore, to obtain impedance matching with the lumped port (generally a 50-Ω feed line), the feed point should be placed at the location where the input impedance of the antenna matches the characteristic impedance of the feed. For the lumped port at a distance x *from* the center of the patch *(or* x_f distance from one of the radiating edges*)*, the input impedance R_{in} of the *RMSA* at resonance can be approximately calculated by either of the two relations [6, 7, 12, 14]

$$R_{in} = R_e \sin^2\left(\frac{\pi x}{L}\right) \qquad for\ 0 \le x \le L/2$$

or

$$R_{in} = R_e \cos^2\left(\frac{\pi x_f}{L}\right) \qquad for\ 0 \le x_f \le L/2 \qquad 4.12$$

where R_e is input resistance at the edge (slot), and it can be computed using Eqn. (*4.16*).

4.2.7 Conductance

Each radiating slot is represented by a parallel equivalent admittance *Y* (with *conductance G* and *susceptance B*). This is shown in Figure 4.3(d). The slots are labeled as #1 and #2. The equivalent admittance of slot #1, based on an infinitely wide, uniform slot, is given by [4]

$$Y_1 = G_1 + jB_1 \tag{4.13}$$

The total admittance at slot #1 (input admittance) is obtained by transferring the admittance of slot #2 from the output terminals to input terminals using the admittance transformation equation of transmission lines. Ideally the two slots should be separated by $\lambda/2$. However, because of fringing effect the length of the patch is electrically longer than the actual length. Therefore, the actual separation of the two slots is slightly less than $\lambda/2$. If the reduction of the length is properly chosen (typically $0.48\lambda < L < 0.49\lambda$), the transformed admittance of slot #2 becomes [4]

$$\widetilde{Y}_2 = \widetilde{G}_2 + j\widetilde{B}_2 = G_1 - jB_1 \tag{4.14}$$

where $\widetilde{G}_2 = G_1$ *and* $\widetilde{B}_2 = -B_1$

Therefore, the total resonant input admittance becomes real and is given by

$$Y_{in} = Y_1 + \widetilde{Y}_2 = 2G_1 \tag{4.15}$$

Since the total input admittance is real at resonant, the input impedance at the edge (slot) R_e is also real, and is given by

$$R_e = \frac{1}{Y_{in}} = \frac{1}{2G_1} \tag{4.16}$$

where $G_1 = 1/R_r$, is slot (edge) conductance and $\boldsymbol{R_r}$ is radiation resistance of the slot.

For better accuracy, the radiation resistance will be given by the following approximations [4, 12]

$$R_r = 120\frac{\lambda_o}{W} \qquad for\ W > 2\lambda_o$$

$$R_r = \frac{1}{\left[\frac{W}{120\lambda_o} - \frac{1}{60\pi^2}\right]} \qquad for\ 0.35\lambda_o < W \leq 2\lambda_o \qquad 4.17$$

$$R_r = 90\left(\frac{\lambda_o}{W}\right)^2 \qquad for\ W \leq 0.35\lambda_o$$

Therefore, the input impedance, $R_{in,}$ of Eqn. (*4.12*) will reduce to

$$R_{in} = \frac{1}{2G_1}\sin^2\left(\frac{\pi x}{L}\right) \qquad for\ 0 \leq x \leq L/2$$

or

$$R_{in} = \frac{1}{2G_1}\cos^2\left(\frac{\pi x_f}{L}\right) \qquad for\ 0 \leq x_f \leq L/2 \qquad 4.18$$

4.2.8 Bandwidth Percentage Approximation

The expressions for approximately calculating the percentage *BW* of the rectangular microstrip antenna in terms of patch dimensions and substrate parameters is given by [12]

$$BW(\%) = \frac{A\,h}{\lambda_o \sqrt{\varepsilon_r}} \sqrt{\frac{W}{L}}$$

where

$$A = 180 \quad for \quad \frac{h}{\lambda_o \sqrt{\varepsilon_r}} \leq 0.045$$

$$A = 200 \quad for \quad 0.045 \leq \frac{h}{\lambda_o \sqrt{\varepsilon_r}} \leq 0.075 \qquad 4.19$$

$$A = 220 \quad for \quad \frac{h}{\lambda_o \sqrt{\varepsilon_r}} \geq 0.075$$

where *W* and *L* are the width and length of the patch and *h* is height of substrate of the *MSA*.

4.3 Conventional Rectangular Microstrip Antenna Design

Now the microstrip antenna is designed for 5 GHz *WLAN* application operating at resonance (central) frequency, f_r, 5.5 GHz. The basic antenna parameters for a *RMSA* are obtained by using Eqns. (*4.1*) through (*4.19*). The dielectric substrate material selected for this design is *RT/Duroid 5880* with $\varepsilon_r = 2.2$, and height *h* is 1.6 mm which is in the range of $0.003\lambda_o \leq h \leq 0.05\lambda_o$. The *RF* signal is feed by using lumped port. Antenna parameters obtained analytically (theoretically) are listed in Table 2.

Table 2 *List of Conventional RMSA parameters and their analytically obtained values.*

Parameters	*Conventional Rectangular MSA*
Operating Frequency,	$f_r = 5.5$ *GHz*
Substrate Height	$h = 1.6$ *mm*
Dielectric Constant	$\varepsilon_r = 2.2$
Conductor type and metallization thickness	*Cu, 18* μm
Effective Permittivity	$\varepsilon_{reff} = 2.036$
Free-space wavelength	$\lambda_o = 54.546$ *mm*
Patch Width, W *Ground Plane Width,* W_g	$W = 21.561$ *mm* $W_g = 31.161$ *mm*
Extension of length and effective length of the patch	$\Delta L = 0.834$ *mm, and* $L_{eff} = 19.114$ *mm*
Patch Length, L *Ground Plane Length,* L_g	$L = 17.446$ *mm* $L_g = 27.046$ *mm*
Lumped port location	$x_f = 6.434$ *mm (or x = 2.289 mm)* $y_f = 10.781$ *mm*
Bandwidth (Approximate value)	*BW = 3.962% (or 217.915 MHz)*

4.4 Bandwidth-Enhanced Rectangular Microstrip Antenna Design

Bandwidth enhancement is achieved using one of the techniques called lowering the quality factor. *MSA* is considered as a high-Q_t, and lowering the value of Q_t by reducing the energy stored around the radiator or increasing losses broadens the bandwidth at its resonance. As shown in Eqns. (*2.21*) and (*2.22*) of section 2.8, Q_t is inversely proportional to substrate height *h* and patch width *W*. Therefore, optimizing the feed point location and keeping all other parameters the same, increasing *h* and *W* to a certain value will lower the value of Q_t, hence the bandwidth will also increase.

Table 3 *List of BW-Enhanced RMSA parameters and their analytically obtained values.*

Parameters	*Bandwidth-enhanced Rectangular MSA*
Operating Frequency,	f_r *= 5.5 GHz (this is kept constant because L is not changing)*
New Substrate Height	*h = 1.95 mm (increasing by 21.875% from initial value of h = 1.6 mm)*
Dielectric Constant	ε_r *= 2.2; (New* ε_{reff} *= 2.035)*
Conductor type and metallization thickness	*Cu, 18 μm*
Free-space wavelength	λ_o *= 54.546 mm*
Patch Width, W *Ground Plane Width,* W_g	*W = 26 mm (increasing by 20.588% from initial value of W = 21.561 mm)* W_g *= 37.7 mm*
Patch Length, L *Ground Plane Length,* L_g	*L = 17.446 mm (kept constant to get the same resonant frequency)* L_g *= 27.046 mm*
Lumped port location	x_f *= 4.2 mm (after optimizing the feed point location)* y_f *= 13 mm (W/2)*
Bandwidth (Approximate value)	*BW = 5.296% (or 291.28 MHz)*

4.5 Coplanar Waveguide Rectangular-Patch Antenna Design

A *CPW-RPA*, as shown in Figure 4.4, consists of a patch surrounded by closely spaced ground conductor on a dielectric substrate, and is then very suitable to *CPW-fed* structure. The patch is formed by widening the center strip conductor of the *CPW*. The feed is a short length of *CPW* which is connected at the center of the patch. The center strip conductor of the *CPW* feed line is

then connected to lumped port which is then attached to the rectangular conductor sheet for termination. The outer conductor of the lumped port is attached to the *CPW* upper ground plane.

The configuration of *CPW* patch antenna itself is actually not a new structure. The structure was first introduced by J. W. Greiser back in 1976, and several research works on the antenna were published. Then, the antenna shown in Figure 4.4 was considered as a loop slot antenna up to recent years; however, after several researches and findings based on intensive electromagnetic field simulations of the structure and experiments on the antenna, the *CPW* patch antenna behaves more like a microstrip patch antenna rather than a loop slot antenna [15, 16].

Hence, taking this into consideration, I have designed a *CPW-RPA* operating at resonant frequency of 5.5 GHz using dielectric substrate of *RT/Duroid 5880* with ε_r = 2.2 with height *h* is 1.95 mm. The *CPW feed* line was designed to be of 50 Ω in order to match the lumped port for maximum power transfer. The parameters of dielectric substrate and geometric dimensions of *CPW-RPA* and its *CPW* feed line length are listed in Table 4.

The fields along the feed side slot and outer side slot are in phase and of almost uniform distribution in the horizontal direction. No field changes to be out of phase along both the input side and outer side slots though an equivalent total length of the slot *W* + *S* at outer side is about $1.6\lambda_0/\sqrt{\varepsilon_r}$, where λ_0 is the wavelength in free space at 5.5 GHz, is longer than one and a half guided wavelength, while the fields along the left and right side slots show an out of phase variation where the equivalent length of the slots $S/2+L+S/2$ is about $0.52\lambda_0/\sqrt{\varepsilon_r}$, close to a distribution of the microstrip patch in mind, the coplanar waveguide patch antenna at the resonant point is much more like a "patch" than a "loop slot". The resonant length of coplanar patch $L \approx 0.47\lambda_0/\sqrt{\varepsilon_r} \approx \frac{1}{2}\lambda_0/\sqrt{\varepsilon_r}$ also follows the same rule as for the microstrip patch antenna. Hence, the antenna shown in Figure 4.4(a) is a "coplanar waveguide patch" antenna not a "loop slot" antenna. Then, analytically we can approximately calculate the width and length of the coplanar waveguide patch using the following relations, respectively [30, 31]

$$W + S \approx 1.6 \frac{\lambda_0}{\sqrt{\varepsilon_r}} \tag{4.20}$$

$$\frac{S}{2} + L + \frac{S}{2} \approx 0.52 \frac{\lambda_0}{\sqrt{\varepsilon_r}} \tag{4.21}$$

where the *CPW rectangular-patch* slot width S is taken to be 1 mm in this particular design.

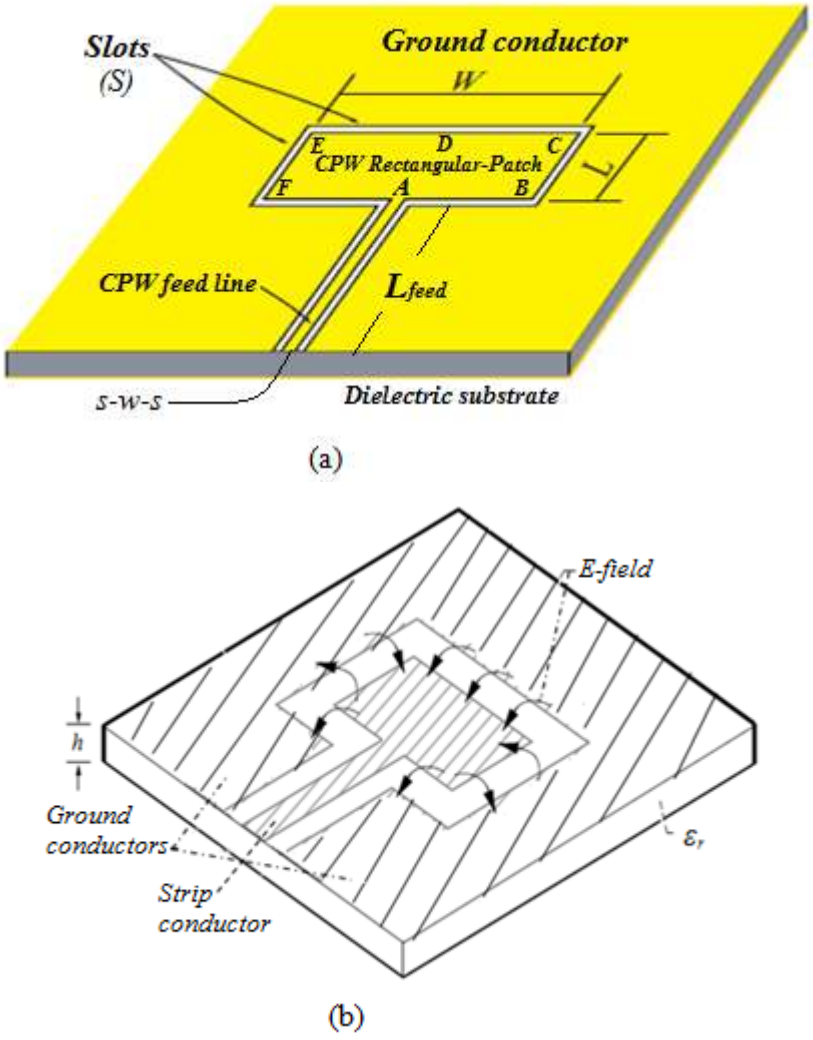

Figure 4.4 *Configuration of CPW antenna: (a) Schematic of CPW-RPA, (b) Electric field distribution along the slots surrounding the patch with a CPW feed line [23, 24, 31].*

Now with the assumption that all conductors are infinitely thin and perfectly conducting, the following equation is used to calculate the *central strip width* (w) of the *CPW feed* line for a given substrate (h, ε_r) and a required characteristic impedance (Z_0) by choosing an appropriate slot width (i.e., *s is taken to be 1 mm*) [32]

$$w \approx s \times 17.368419 \left[\frac{\left(Z_0 / \eta_0 \right)^{-1.327162}}{\left(\varepsilon_r + 1.017967 \right)^{6.631557}} \right] \left[\left(\frac{s}{h} \right)^{-0.645743} \left(\frac{Z_0}{\eta_0} \right)^{2.274152} + \frac{1.998984 \left(\frac{s}{h} \right)^{0.172677}}{\left(\varepsilon_r + 1.09 \right)^{1.106353}} \right]^{-5.38965} + \frac{0.047079}{\left(\frac{s}{h} \right)^{1.163113}} \qquad 4.22$$

where Z_0 is usually taken to be 50 ohm, and $\eta_0 = 120\pi$.

The *CPW feed* line length (L_{feed}) is approximately given by [30, 31]

$$L_{feed} \approx 0.5 \lambda_g = 0.5 \frac{\lambda_0}{\sqrt{\varepsilon_r}} \qquad 4.23$$

Table 4 *List of CPW-RPA parameters and their analytically obtained values.*

Parameters	*CPW Rectangular-Patch Antenna*
Operating frequency,	f_r = 5.5 GHz
Substrate height	h = 1.95 mm
Dielectric constant	ε_r = 2.2
Effective permittivity	$\varepsilon_{reff} \approx 1.6$
Conductor type and metallization thickness	*Cu, 18 μm*
Free-space wavelength	λ_o = 54.546 mm
CPW feed line	*s-w-s: (1.0-1.6-1.0) mm*
L_{feed}	*18 mm*
CPW rectangular-patch	*L = 17.25 mm* *W = 57 mm* *S = 1.0 mm*

CHAPTER 5

Simulation Results and Discussion

5.1 Simulation

The designed antenna was drawn into *EMPIRE*^{TM} *XCcel* simulation software of version 5.4 in order to analyze the theoretical computational results obtained for each antenna type. The simulation software used finite-difference time-domain method to analyze the antennas. *FDTD* technique computes the fields on the structure in the time domain. This method handles moderate-sized structures and readily includes complex material properties such as biological features. *FDTD* divides the region into *cubic cells* and when excited by pulse feeding functions, it produces wide frequency bandwidth responses. The *FDTD* method solves the coupled Maxwell's curl equations directly in the time domain by using finite time steps over small cells in space. The method reduces the differential equations to difference equations that can be solved by sets of simple equations. The method alternates between the electric and magnetic fields solved at locations a half-step apart because central differences are used to approximate derivatives [14].

5.2 Simulation Results

Tables 2, 3 and 4 contain lists of theoretically obtained antenna parameters and we used them to draw the configurations of conventional *RMSA*, bandwidth-enhanced *RMSA* and *CPW* rectangular-patch antenna into the simulation software, respectively. Each antenna is then simulated at resonant frequency and their output results are presented below.

A) Physical Structure

The 2D and 3D views from GANYMEDE editor of Empire simulator shows layout of the general physical structures of each antenna as shown below.

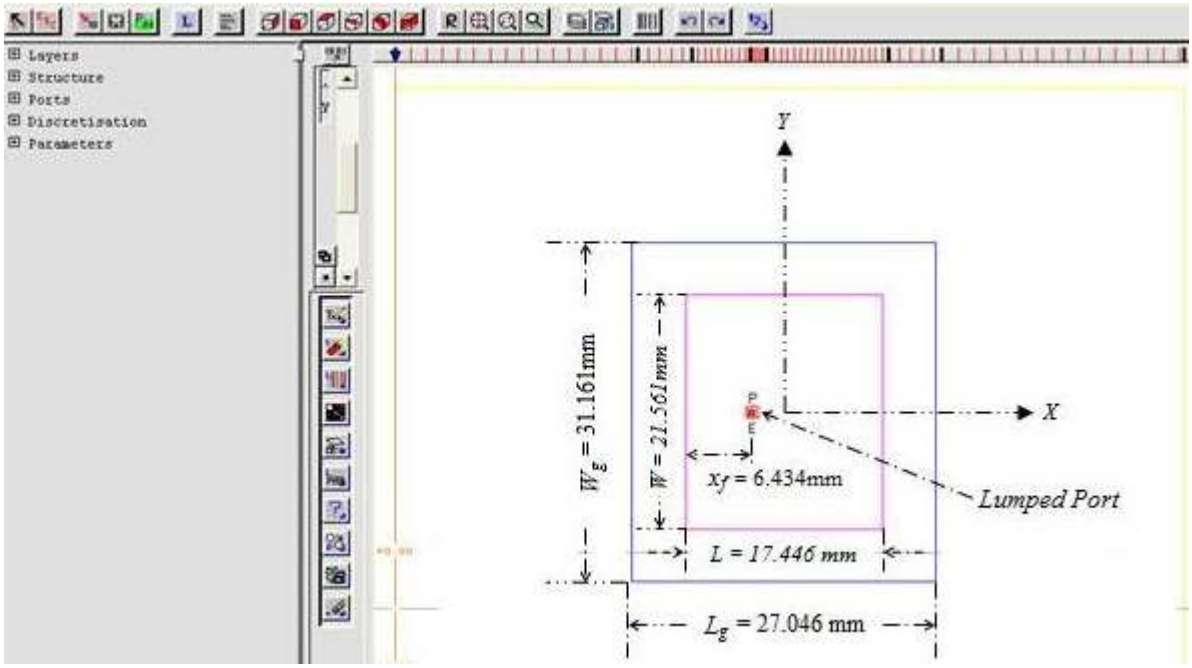

(a)

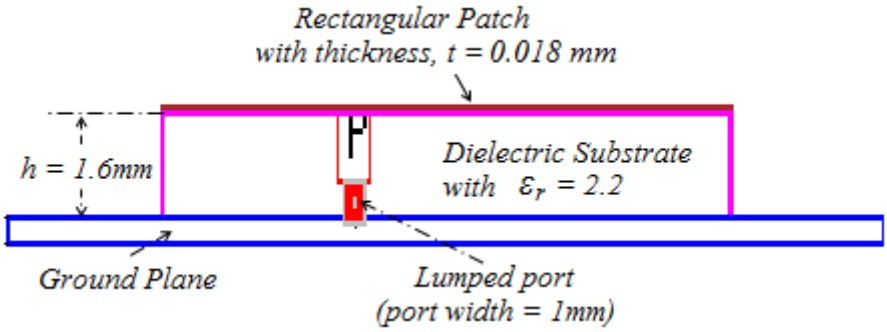

(b)

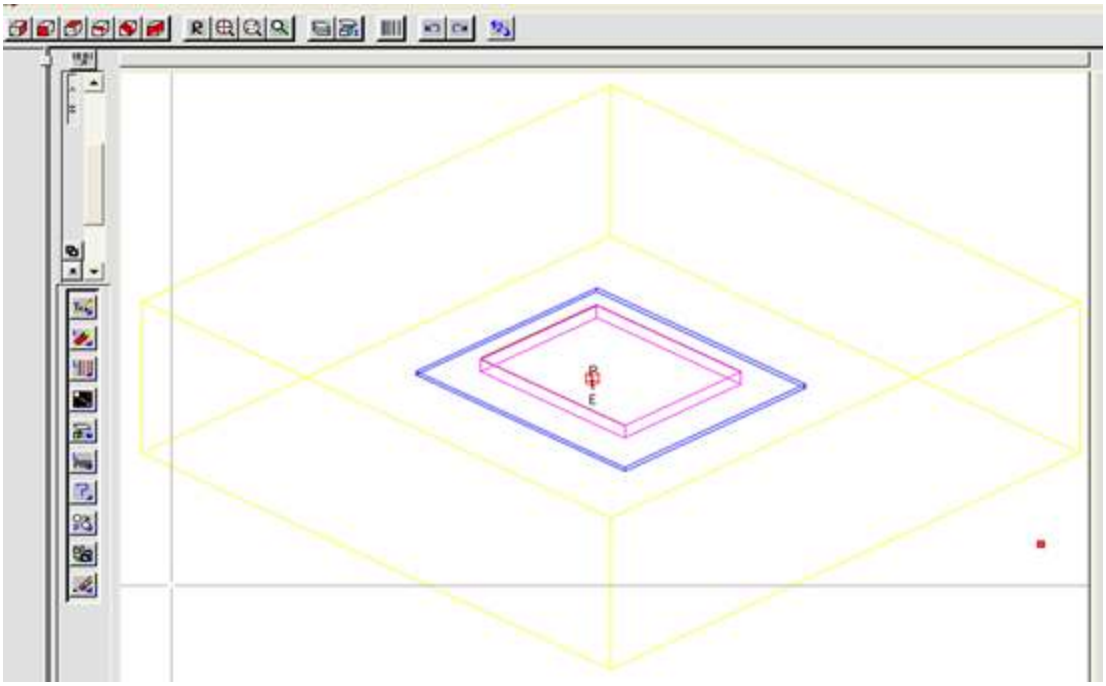

(c)

Figure 5.1 ***Conventional RMSA structure****: (a) 2D-top view, (b) 2D-side view, (c) 3D-view.*

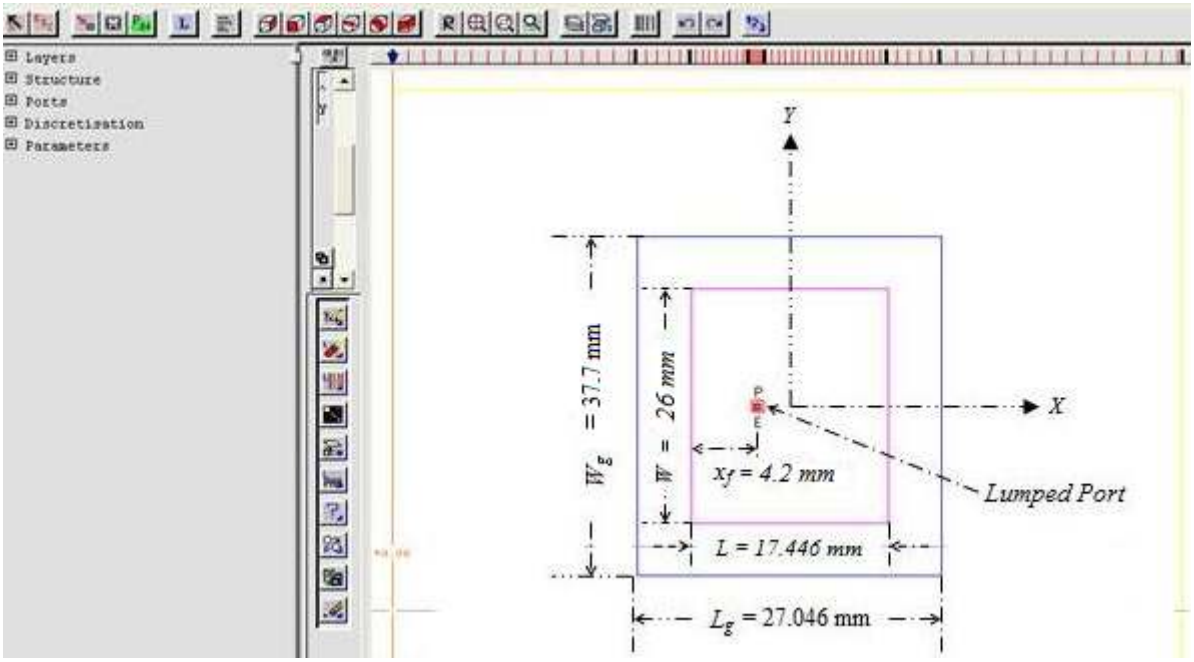

(a)

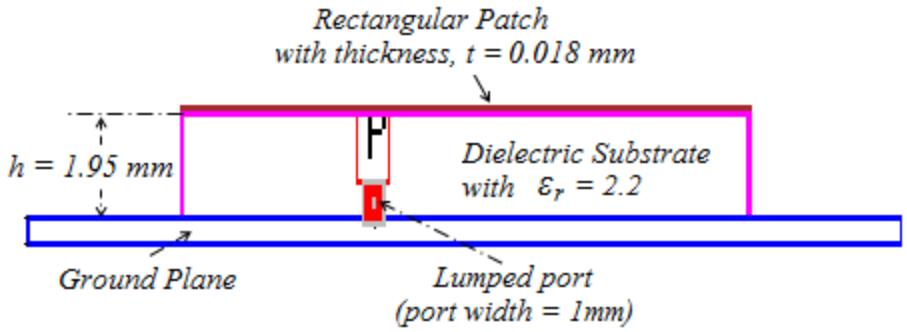

(b)

Figure 5.2 ***BW-Enhanced RMSA structure****: (a) 2D-top view, (b) 2D-side view.*

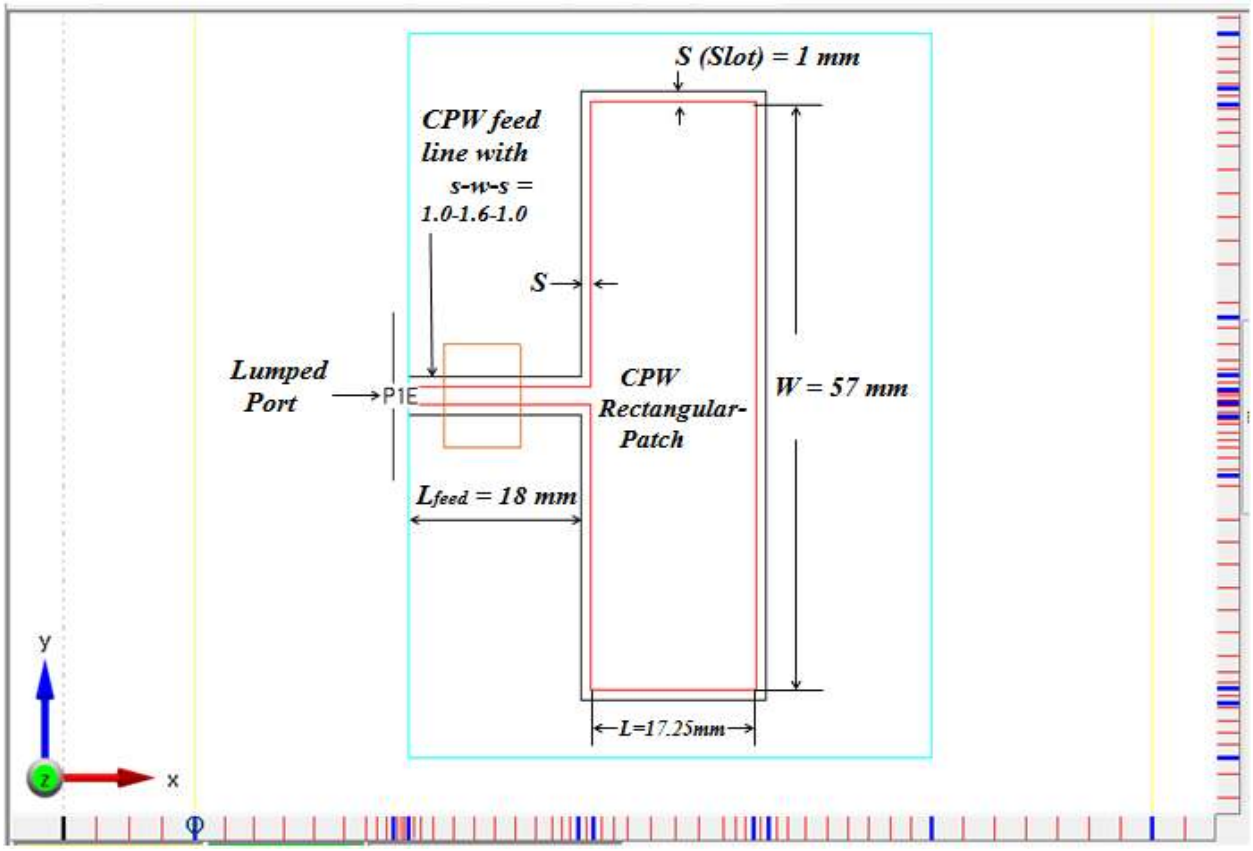

(a)

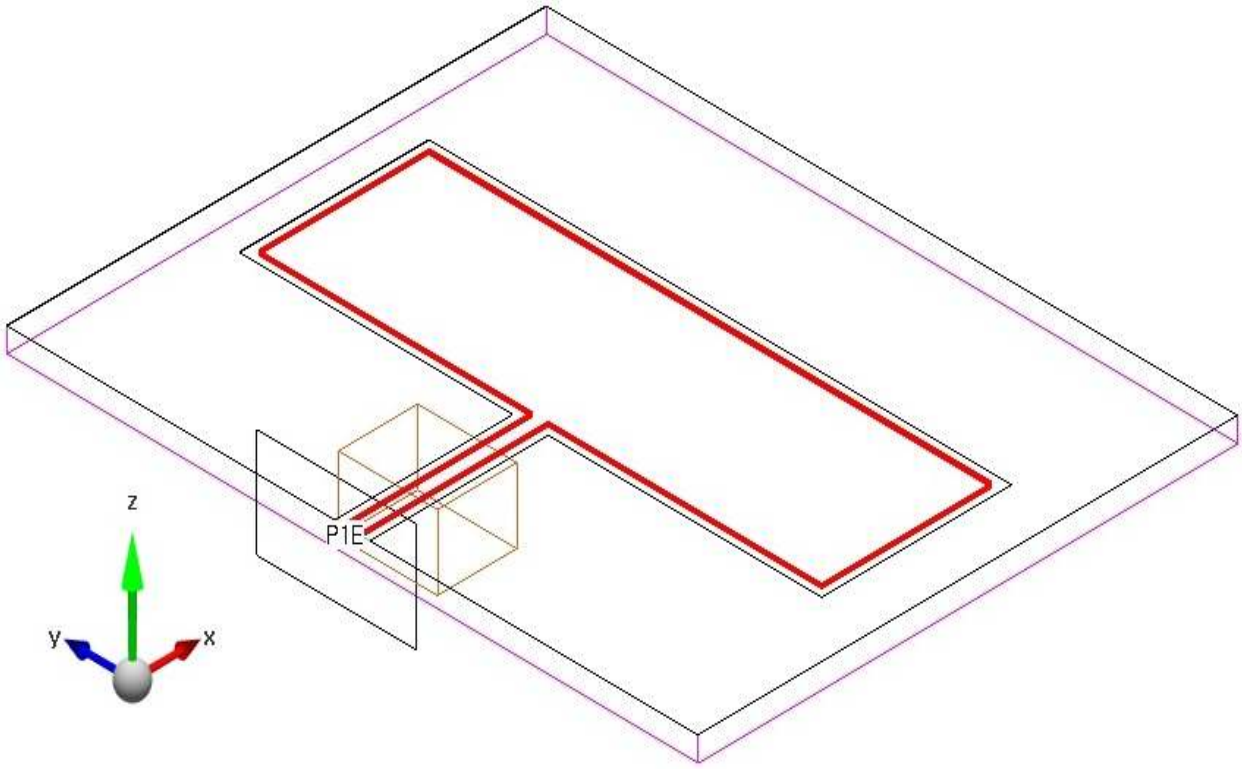

(b)

Figure 5.3 ***CPW-RPA structure****: (a) 2D- top view, (b) 3D- view.*

B) VSWR and Return Loss

Here the simulation results show that the antenna *BW* can be obtained either from the 2:1 *VSWR* plot or from the *RL*, S_{11}, plots. The f_r of the antenna is obtained at 5500 MHz. The antenna bandwidths obtained are: ***196.5776 MHz*** (i.e., ***3.574%***), ***315.341 MHz*** (i.e., ***5.734%***) and ***384.2327 MHz*** (i.e., ***6.986%***) for *conventional RMSA*, *BW-Enhanced RMSA* and *CPW-RPA*, respectively.

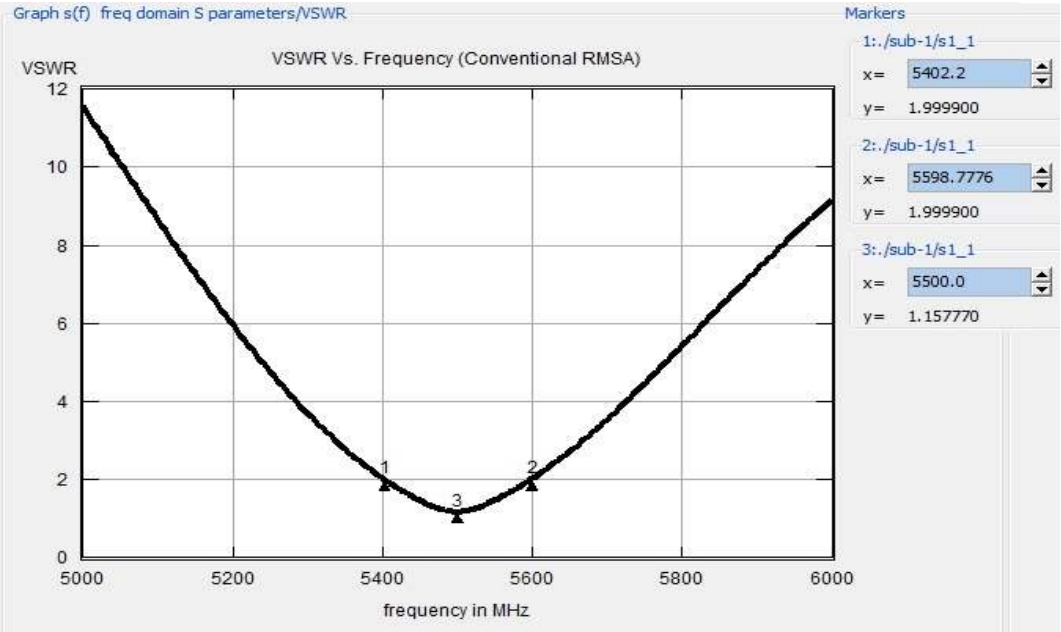

(a)

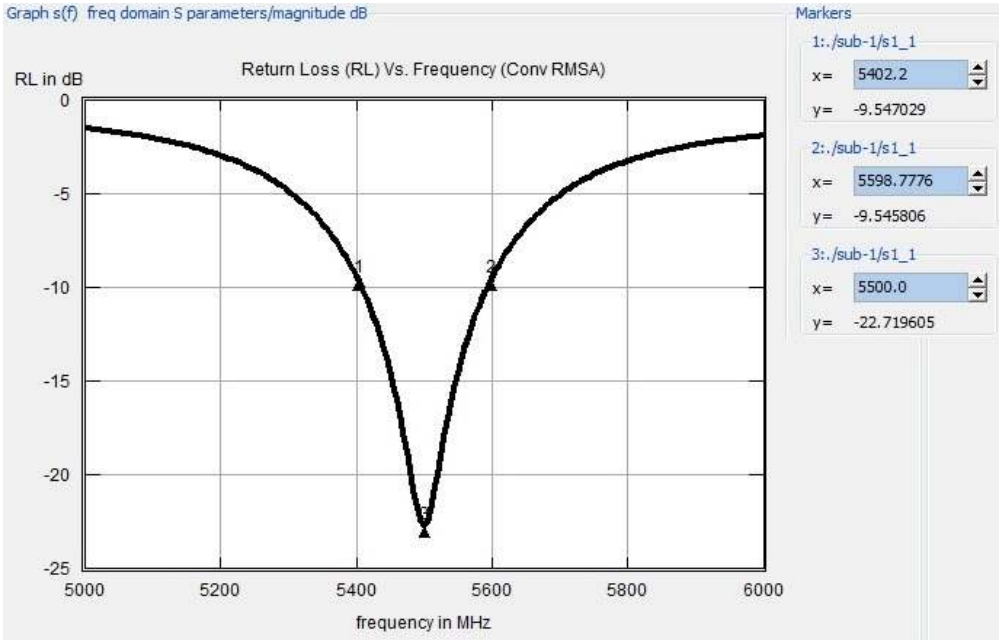

(b)

Figure 5.4 ***Conventional RMSA*** *(a) VSWR versus frequency graph; (b) S_{11} versus frequency graph: from both graphs (#1) shows f_l = 5402.2 MHz; (#2) shows f_u =5598.7776 MHz; and (#3) shows resonance frequency f_r =5500 MHz.*

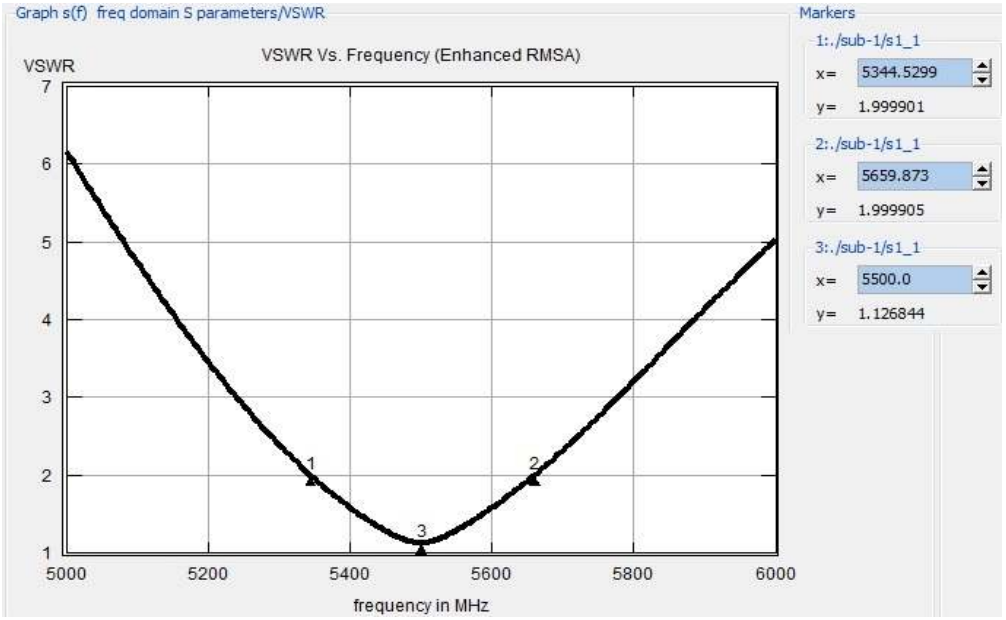

(a)

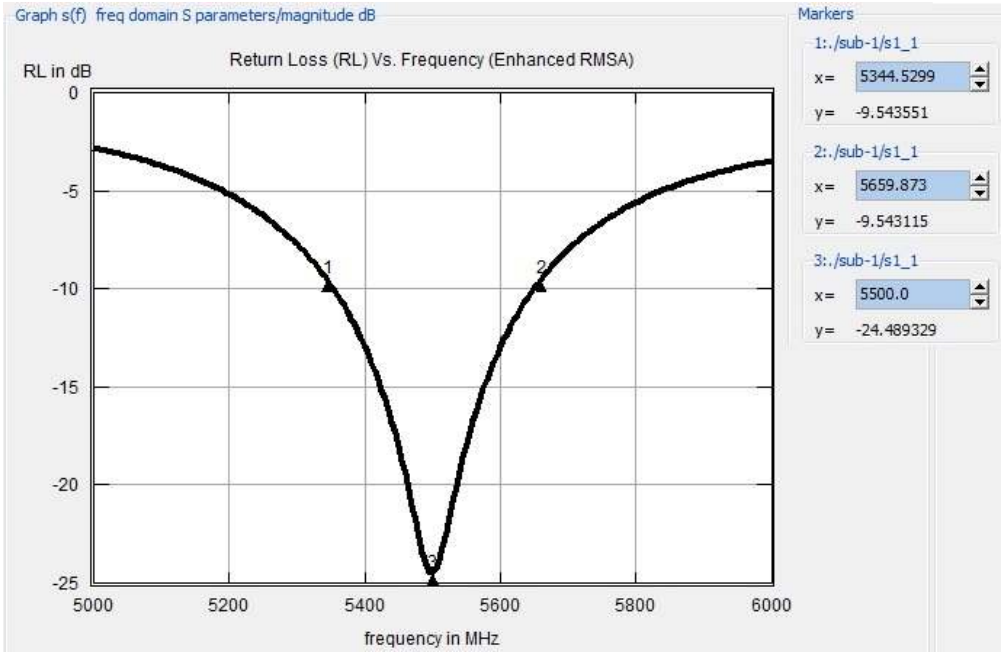

(b)

Figure 5.5 ***BW-Enhanced RMSA*** *(a) VSWR versus frequency graph; (b) S_{11} versus frequency graph: from both graphs (#1) shows f_l = 5344.5299 MHz; (#2) shows f_u =5659.873 MHz; and (#3) shows resonance frequency f_r =5500 MHz.*

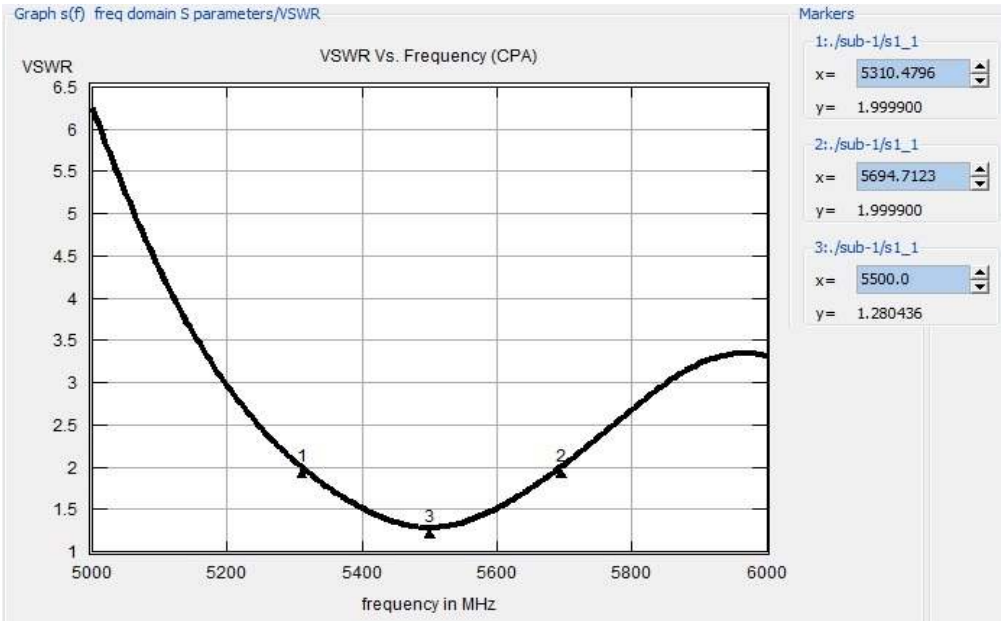

(a)

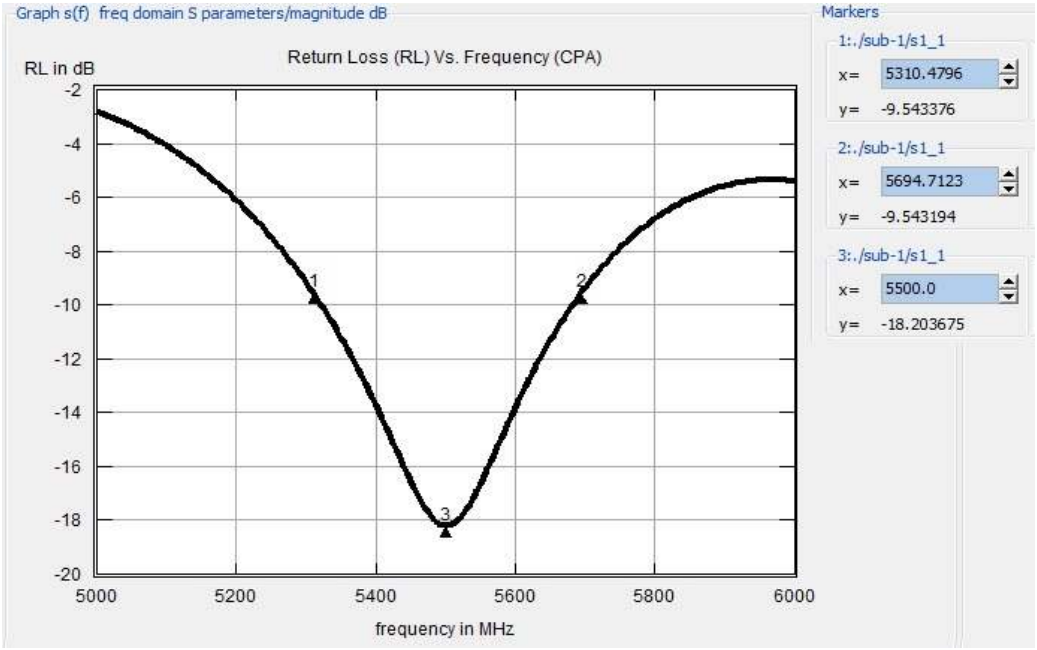

(b)

Figure 5.6 ***CPW-RPA*** *(a) VSWR versus frequency graph; (b) S_{11} versus frequency graph: from both graphs (#1) shows f_l = 5310.4796 MHz; (#2) shows f_u =5694.7123 MHz; and (#3) shows resonance frequency f_r =5500 MHz.*

C) Smith Chart Plot

The smith chart in polar plot shows the relationship between *input impedance versus frequency variation* and the *VSWR circle*. The two points $Z_{in(1)}$ and $Z_{in(2)}$ are the input impedance values of the antenna where input impedance curve intersects with the *VSWR = 2* circle on the smith chart. These points indicate the lower (f_l) and upper (f_u) frequencies that are used to calculate the *BW*.

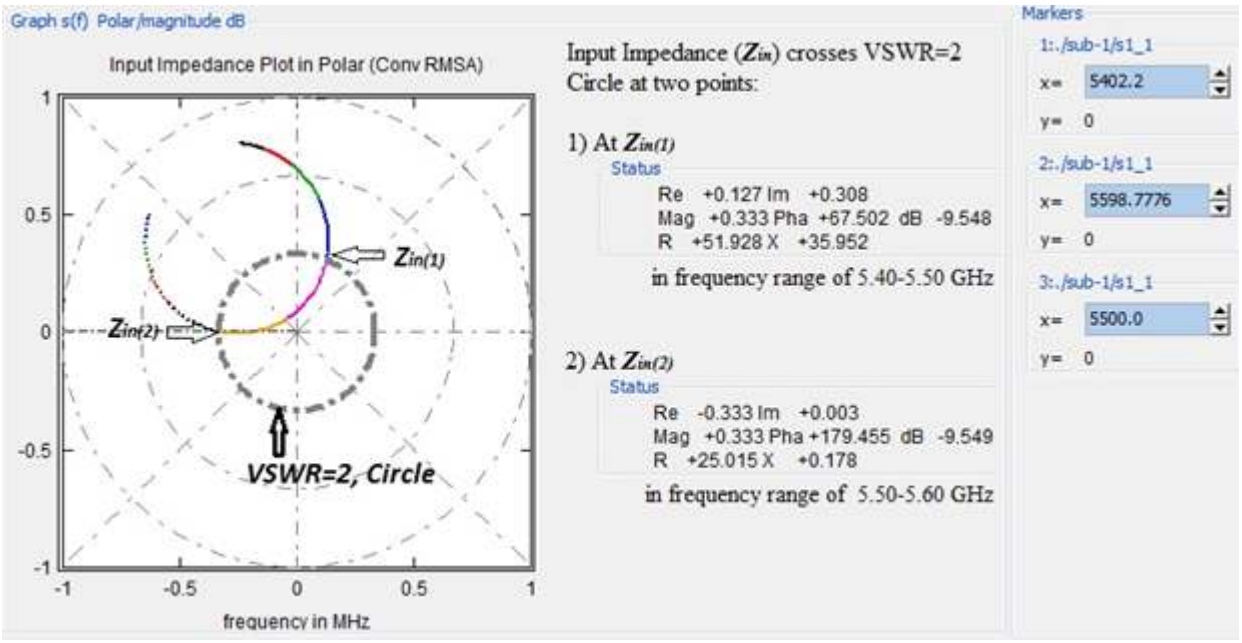

Figure 5.7 *Conventional RMSA*: *Smith chart plot in polar.*

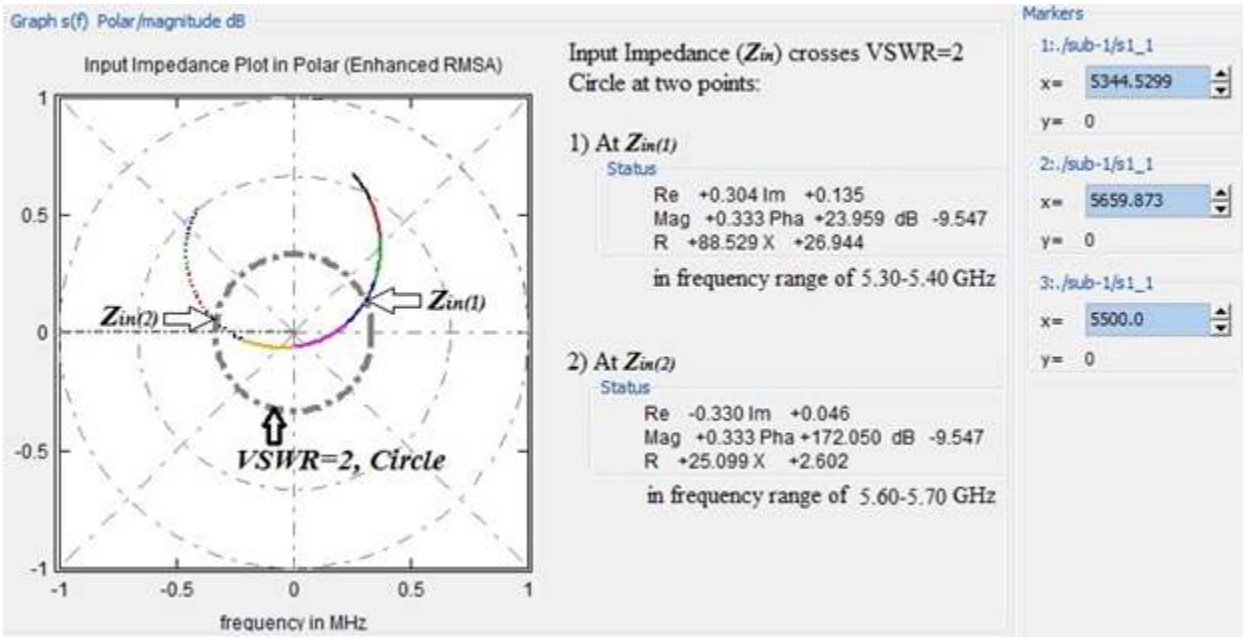

Figure 5.8 ***BW-Enhanced RMSA*****:** *Smith chart plot in polar.*

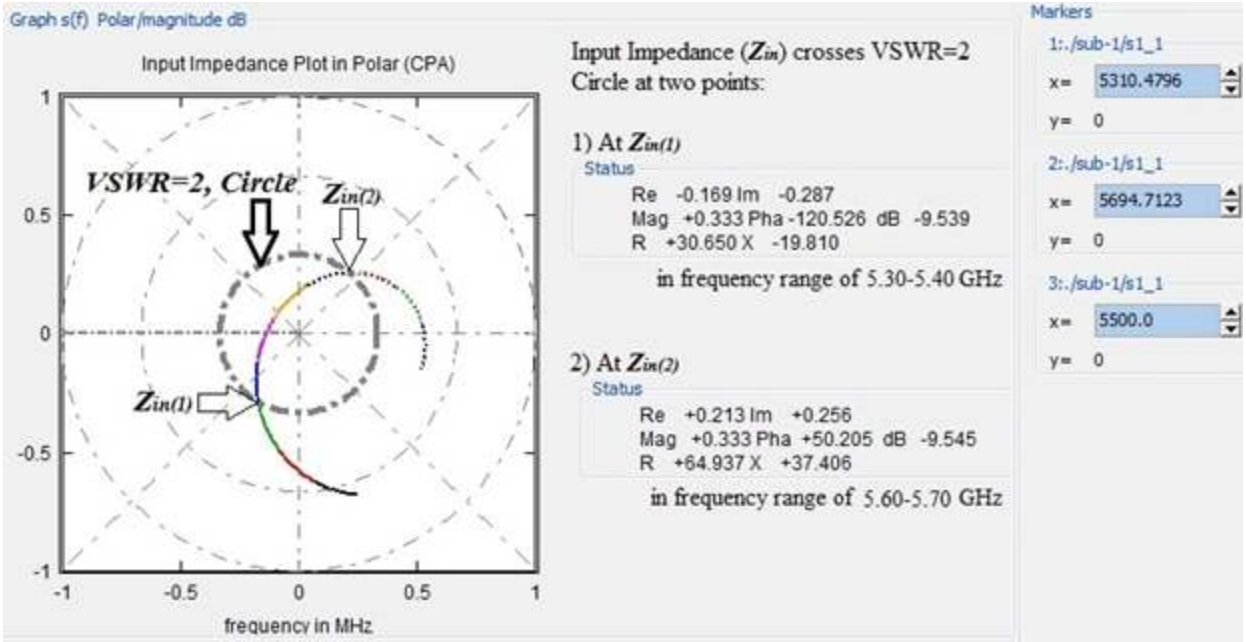

Figure 5.9 ***CPW-RPA*****:** *Smith chart plot in polar.*

D) Radiation Pattern and Gain

The field radiates normal to its patch surface in the broadside direction. The elevation angel was taken from θ: *0 to* π degrees and the azimuth angel must be fixed (i.e.; it could be taken either at taken at $\Phi=0$ or $\Phi=\pi/2$ degree. Hence, I took $\Phi = 0$ to plot the radiation pattern.

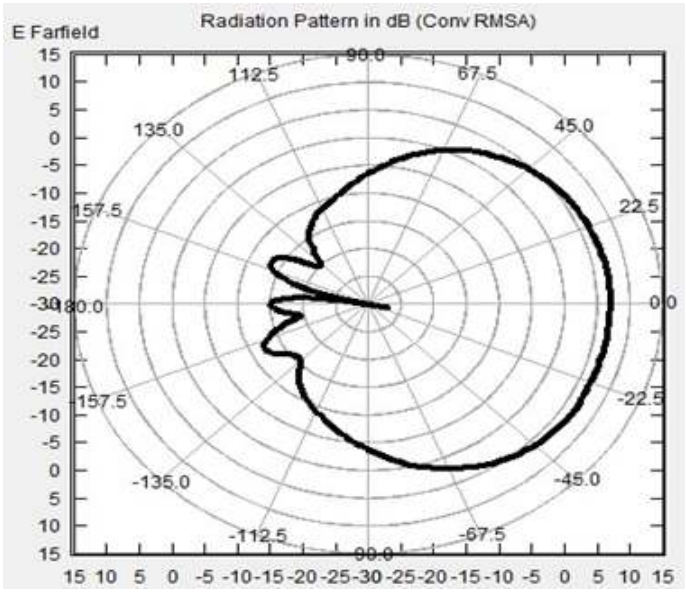

(a)

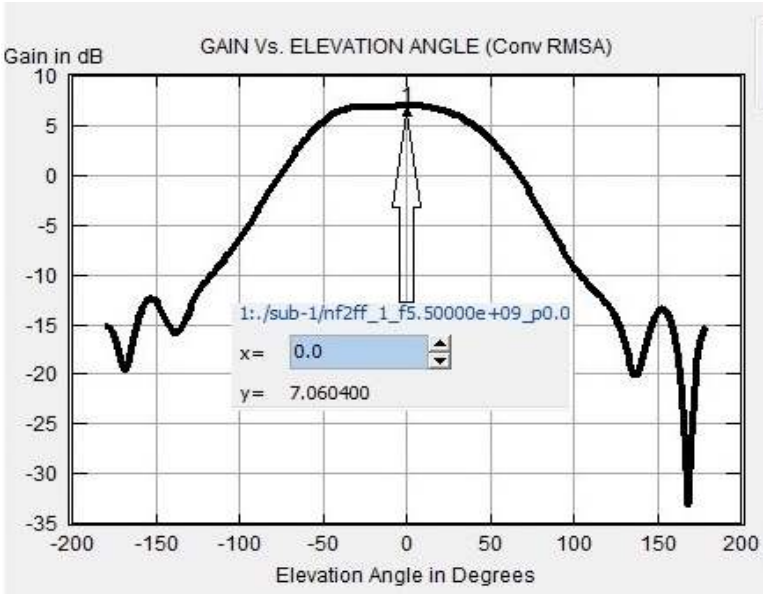

(b)

Figure 5.10 ***Conventional RMSA****: (a) Radiation pattern; (b) Gain (****7.0604 dB****).*

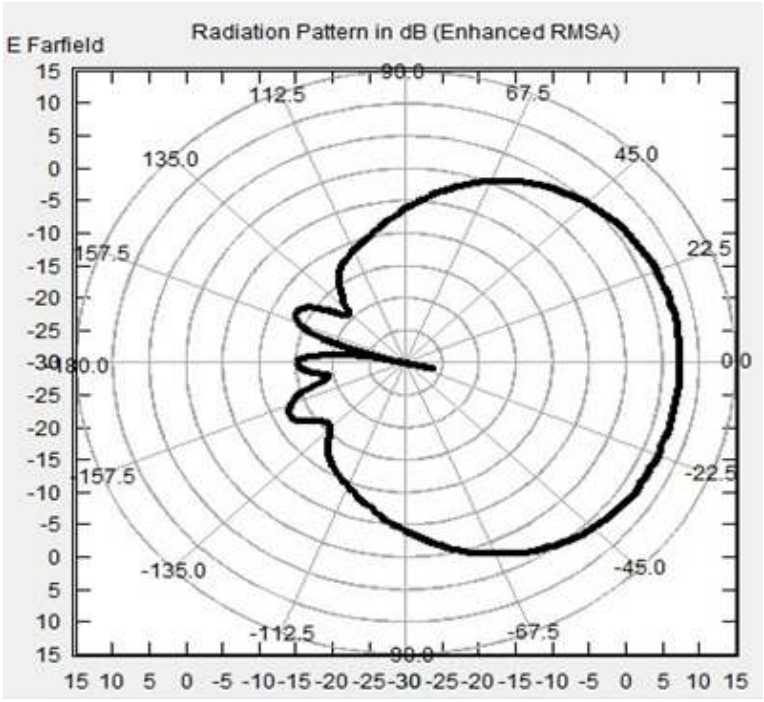

(a)

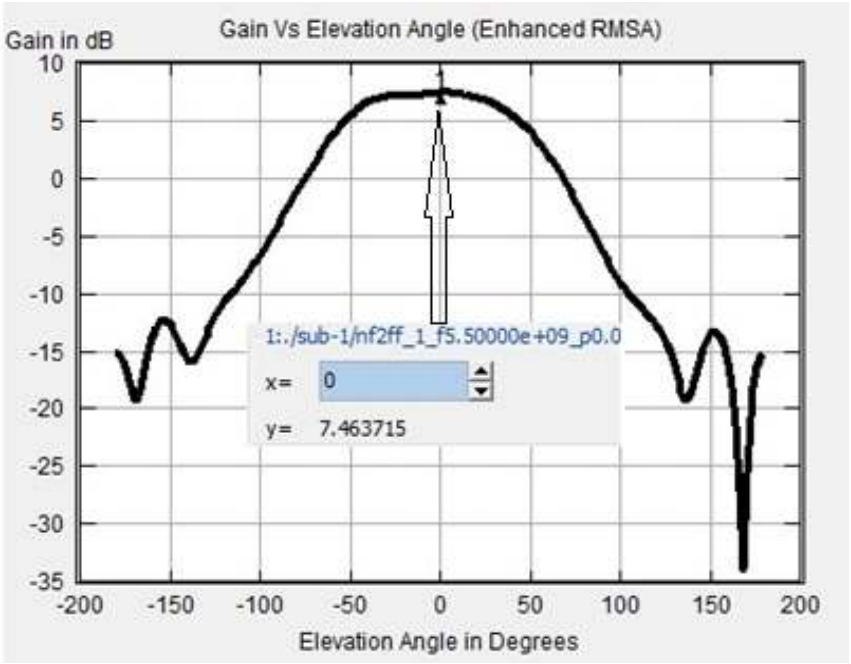

(b)

Figure 5.11 ***BW-Enhanced RMSA****: (a) Radiation pattern; (b) Gain (****7.463715 dB****).*

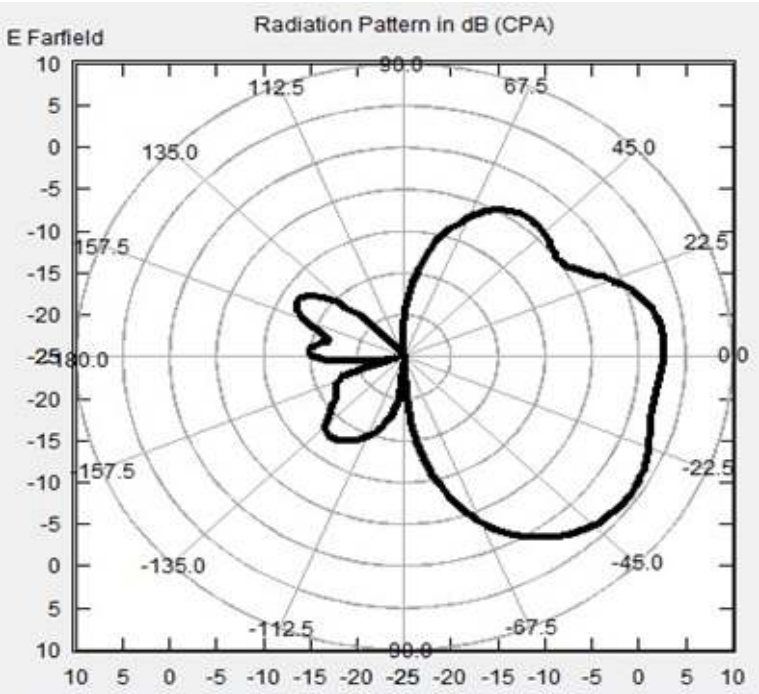

(a)

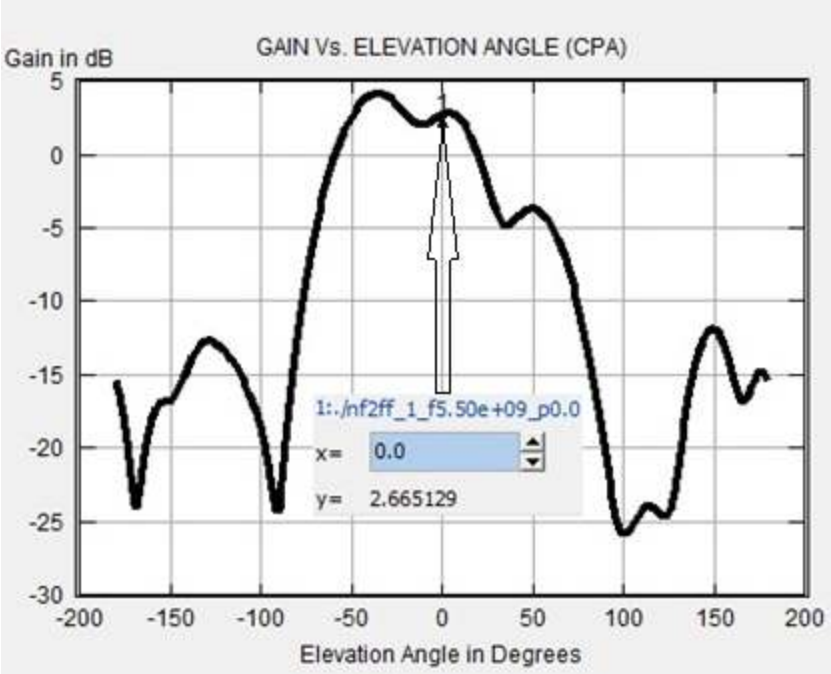

(b)

Figure 5.12 ***CPW-RPA****: (a) Radiation pattern; (b) Gain (****2.665129 dB****).*

E) Near and Far Fields

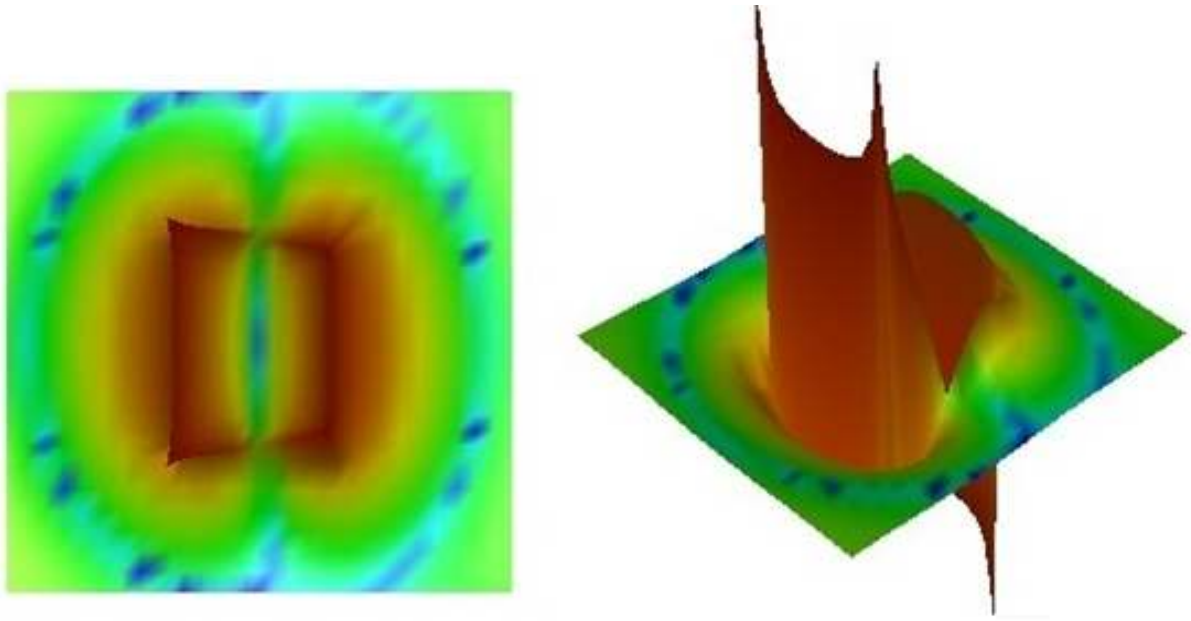

(a)

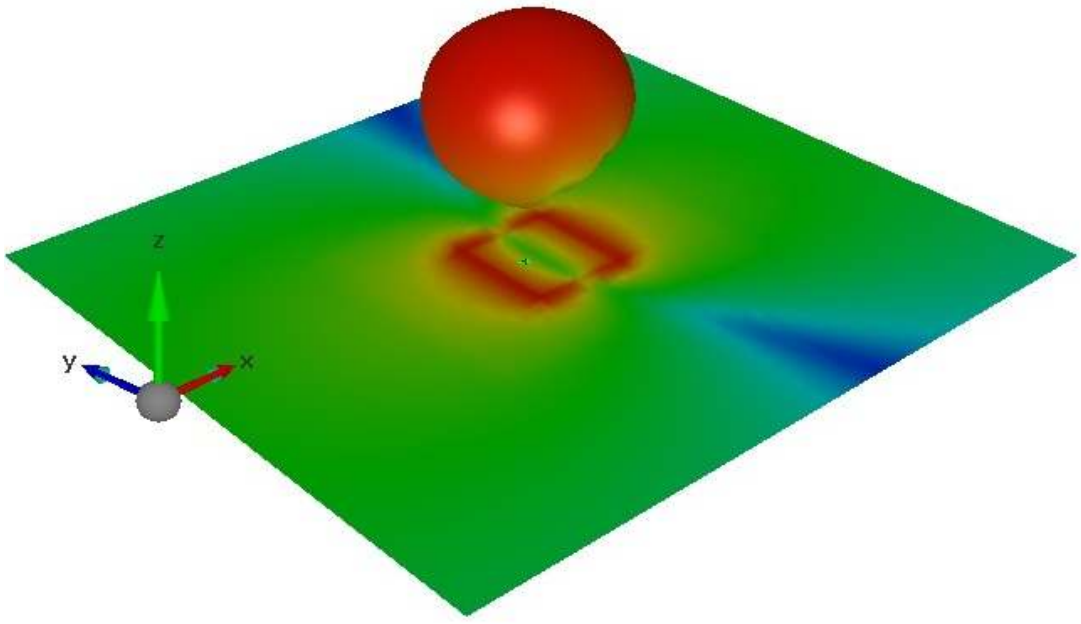

(b)

Figure 5.13 ***Conventional RMSA****: (a) current distribution and near field (E_z) distribution with antenna geometry; (b) far field 3D radiation pattern.*

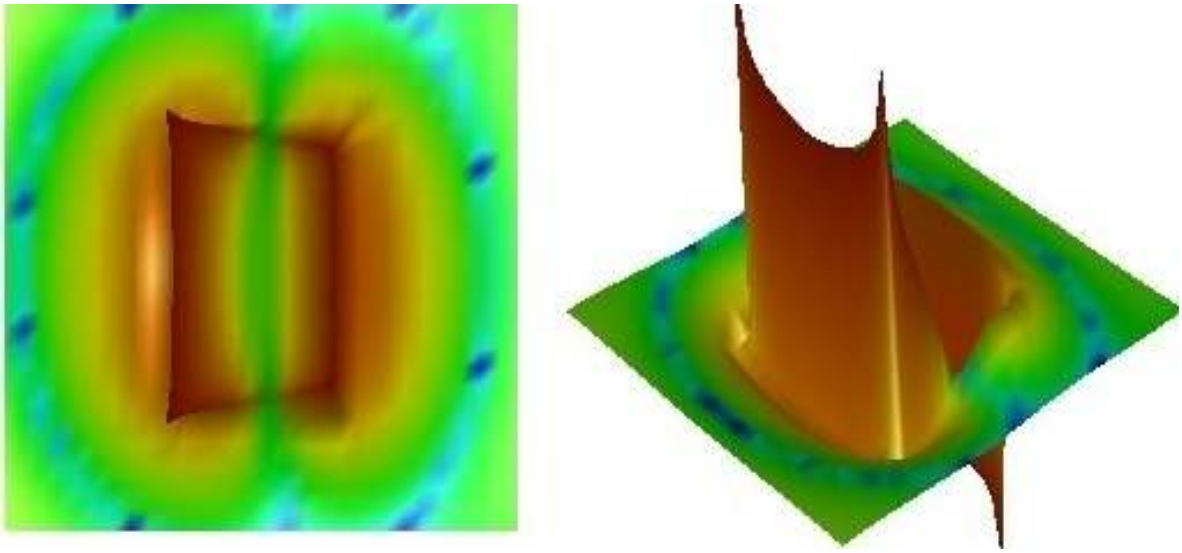

(a)

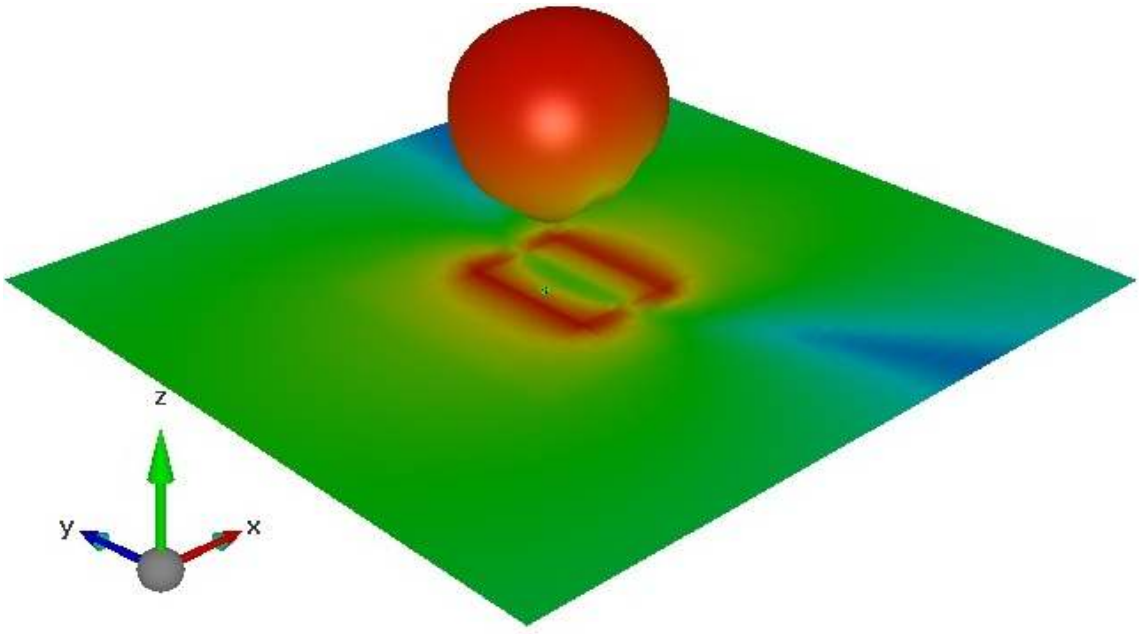

(b)

Figure 5.14 ***BW-enhanced RMSA****: (a) current distribution and near field (E_z) distribution with antenna geometry; (b) far field 3D radiation pattern.*

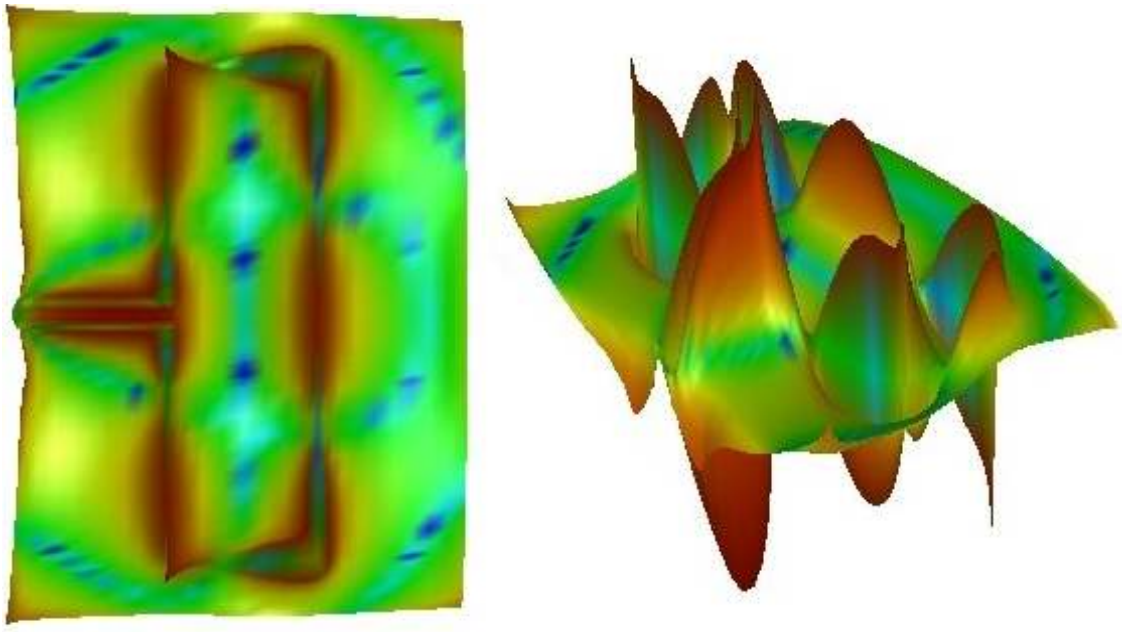

(a)

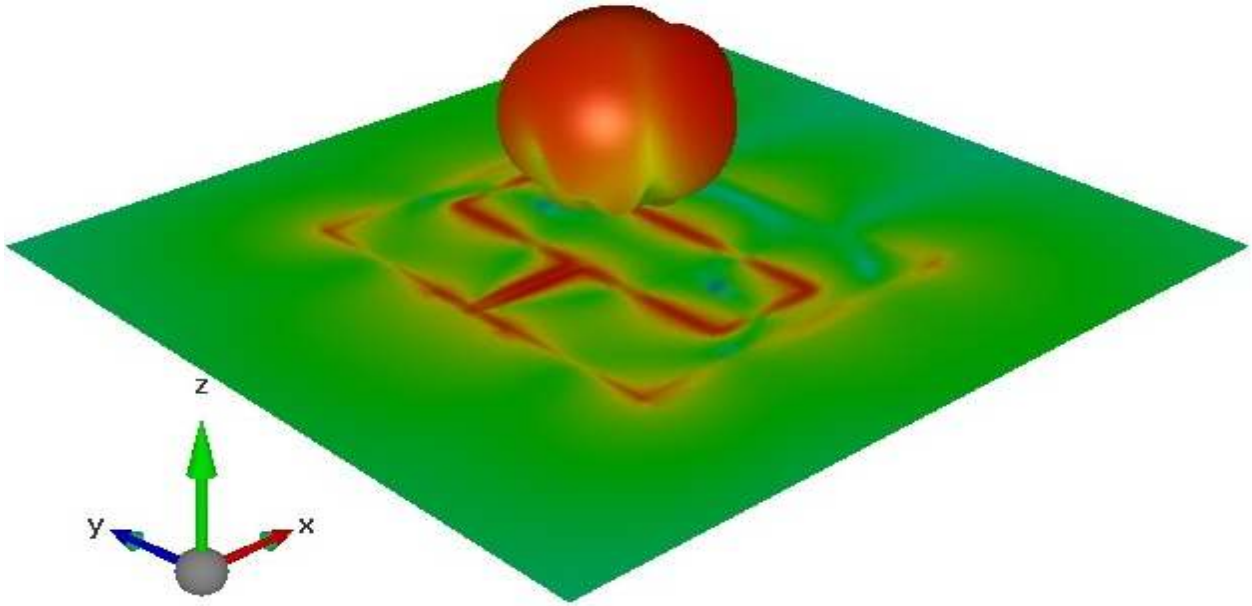

(b)

Figure 5.15 ***CPW-RPA****: (a) current distribution and near field (E_z) distribution with antenna geometry; (b) far field 3D radiation pattern.*

F) Impedance and Admittance

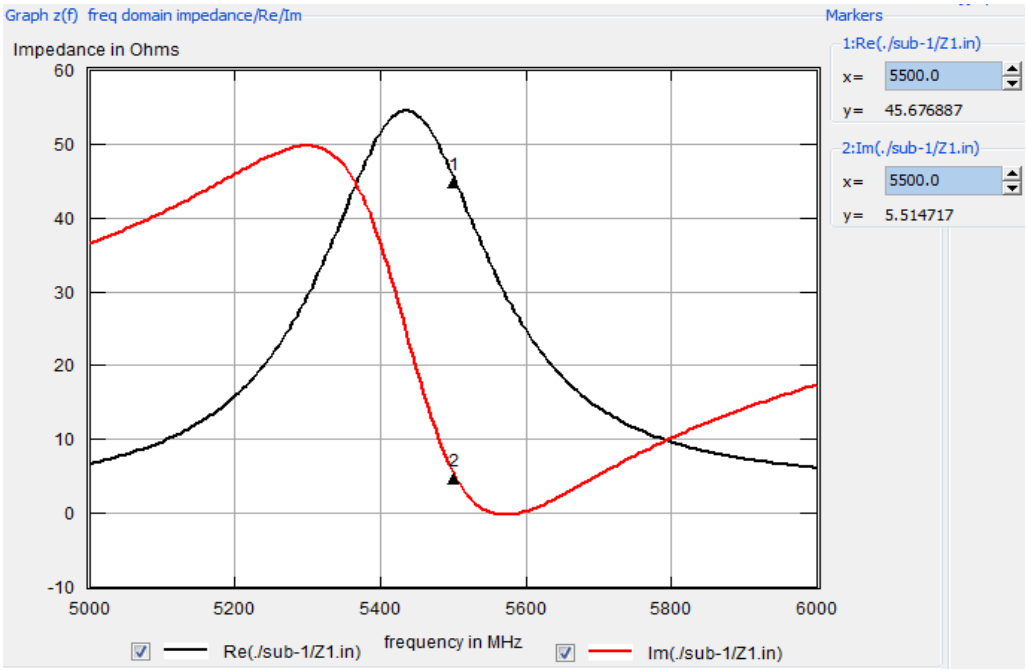

(a)

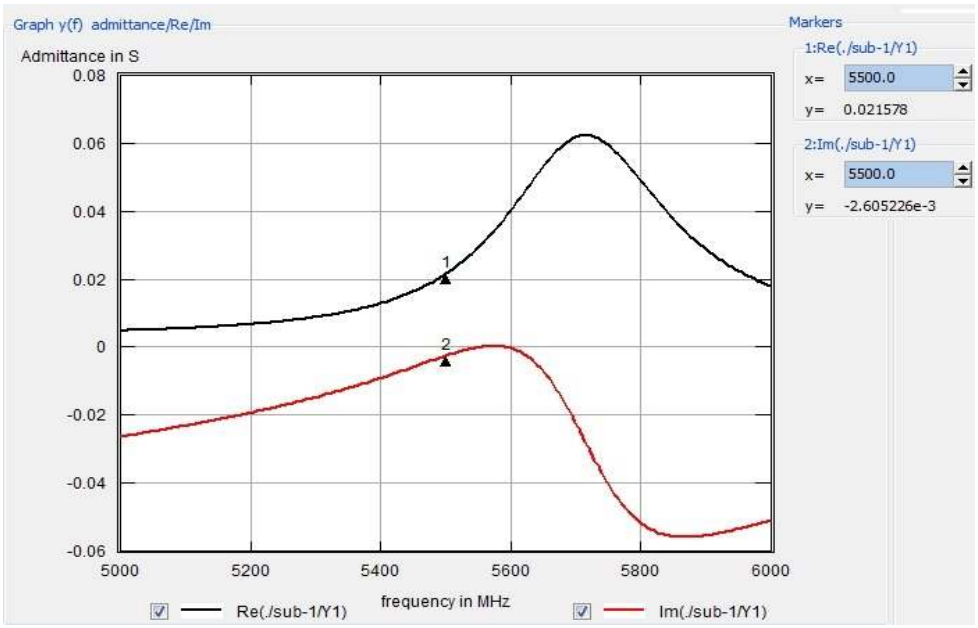

(b)

Figure 5.16 ***Conventional RMSA:*** *Impedance and Admittance variations with frequency.*

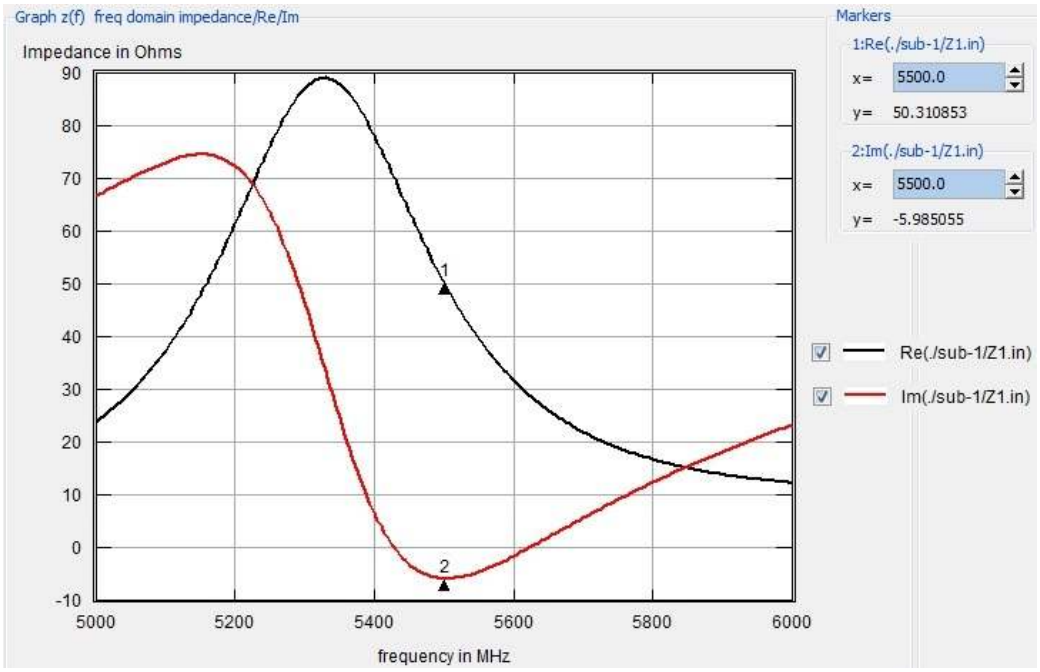

(a)

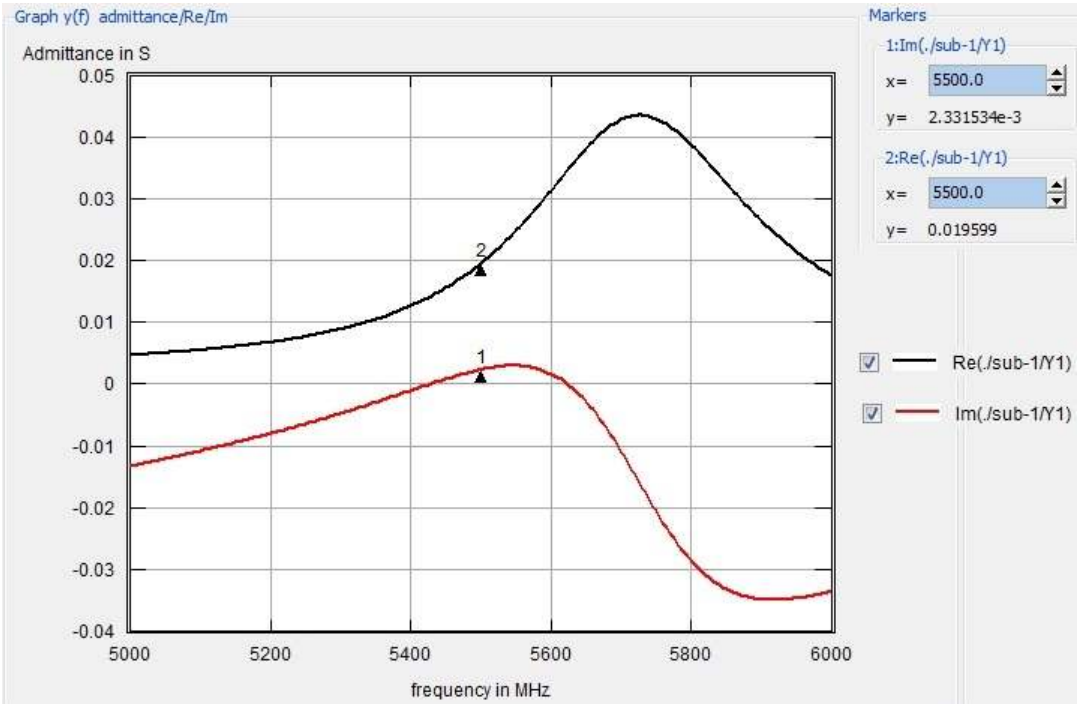

(b)

Figure 5.17 ***BW-Enhanced RMSA:*** *Impedance and Admittance variations with frequency.*

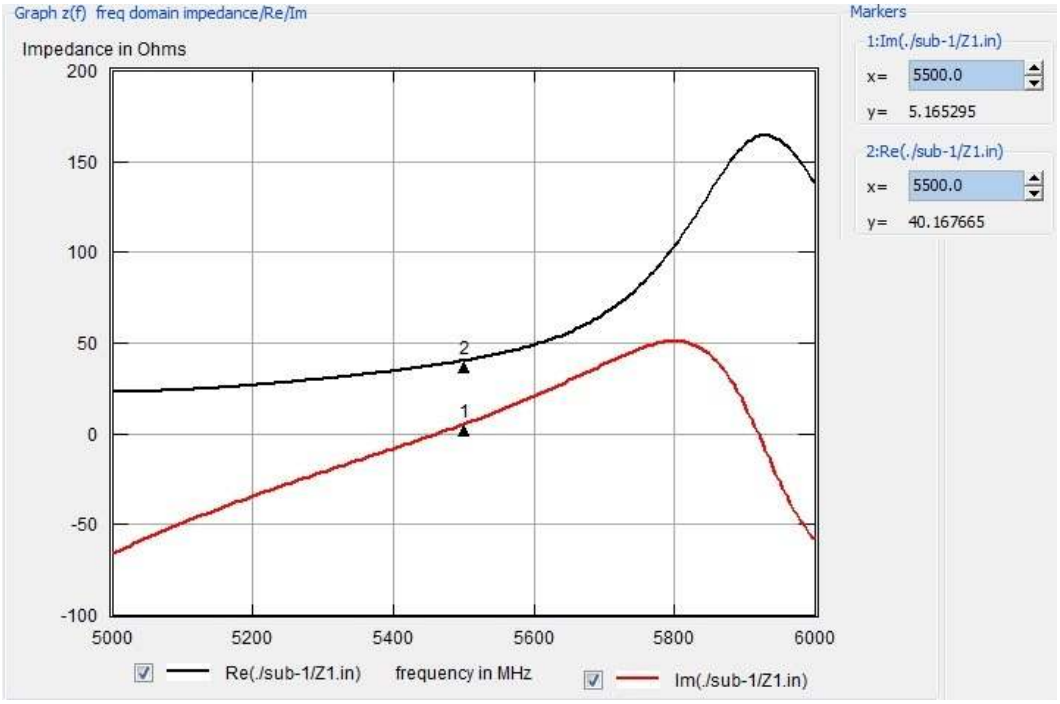

(a)

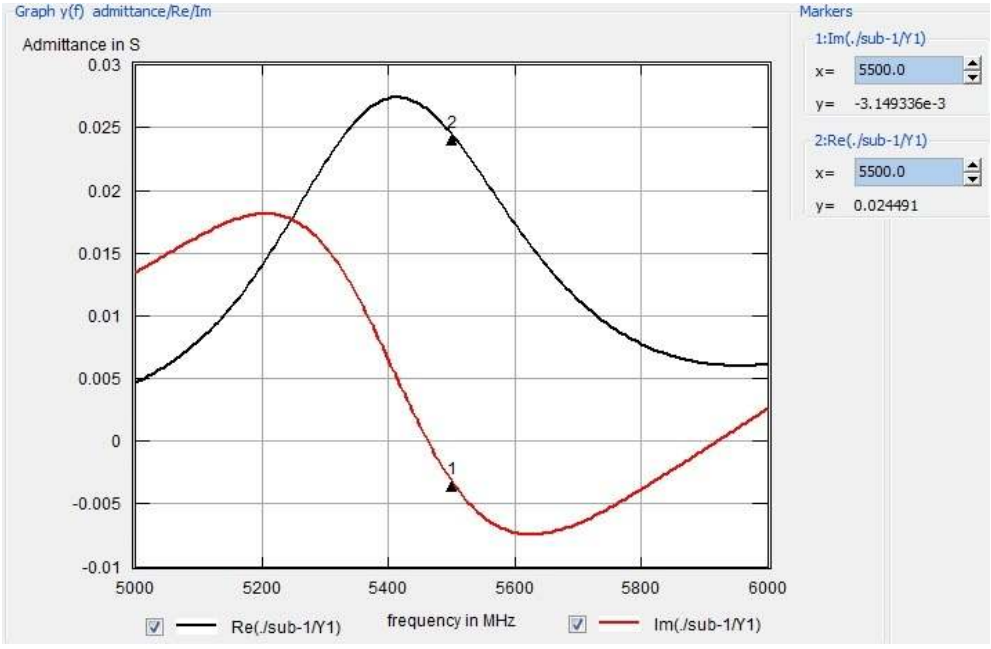

(b)

Figure 5.18 ***CPW-RPA:*** *Impedance and Admittance variations with frequency.*

G) Simulation details

For Conventional RMSA

```
This is ff V 5.40 (C) IMST GmbH 2002-2010

Phi is fixed, Phi= 0.0  Deg
Warning: switching off Mirror at zmin
Frequency f=5.500000000000000e+009 Hz
 Normalization:  Gain        Port 1

          Power into excitation port is P_in     = 1.000000000000000e+000
 Incident Power into excitation port is P_in_inc = 1.005374864432344e+000
          Radiated power              is P_rad    = 9.711925825349010e-001
 Excitation port is 1
 Antenna   Efficiency (P_rad/P_in)     is 97.119 %
 Radiation Efficiency (P_rad/P_in_inc) is 96.600 %
   Power at xmin is 1.177246513850474e-001 ( 12.122 %), IMAG -9.392622533101202e-003 (  -0.967 %)
   Power at xmax is 6.489871066355943e-002 (  6.682 %), IMAG -7.653089224712904e-003 (  -0.788 %)
   Power at ymin is 3.986594163182074e-002 (  4.105 %), IMAG 9.481084669338327e-003 (   0.976 %)
   Power at ymax is 3.983866154220440e-002 (  4.102 %), IMAG 9.465263994014230e-003 (   0.975 %)
   Power at zmax is 7.088646173122690e-001 ( 72.989 %), IMAG -1.374904601805354e-002 (  -1.416 %)
farfield processing: 100.00 % done.
***  Simulation  for RecPatchForThesisWithHomeEmpireWithFeedLine done


Status
 0      Errors,          1    Warning
 15000  Steps , 3.58 ms each,     Performance 37.968 MCells/s

 Energy estimate E  2.38692e-003 / max 3.43022e+000 / decrement    63 dB
 Energy estimate H  1.62641e-003 / max 6.04159e+000 / decrement    71 dB

 Time 00:57, 00:00 to go (estimated)
```

For BW-enhanced RMSA

```
This is ff V 5.40 (C) IMST GmbH 2002-2010

Phi is fixed, Phi= 0.0  Deg
Warning: switching off Mirror at zmin
Frequency f=5.500000000000000e+009 Hz
 Normalization:  Gain_Inc    Port 1

          Power into excitation port is P_in     = 9.964431376879769e-001
 Incident Power into excitation port is P_in_inc = 1.000000000000000e+000
          Radiated power              is P_rad    = 9.979498669566036e-001
 Excitation port is 1
 Antenna   Efficiency (P_rad/P_in)     is 100.151 %
 Radiation Efficiency (P_rad/P_in_inc) is 99.795 %
   Power at xmin is 1.139193755287880e-001 ( 11.415 %), IMAG -9.499912630285753e-003 (  -0.952 %)
   Power at xmax is 6.642306481714620e-002 (  6.656 %), IMAG -8.185257785606517e-003 (  -0.820 %)
   Power at ymin is 4.061597806358199e-002 (  4.070 %), IMAG 8.869717535943508e-003 (   0.889 %)
   Power at ymax is 4.059034486127822e-002 (  4.067 %), IMAG 8.854319932082924e-003 (   0.887 %)
   Power at zmax is 7.364011036858092e-001 ( 73.791 %), IMAG -1.500375541671000e-002 (  -1.503 %)
farfield processing: 100.00 % done.
***  Simulation  for RecPatchForThesisWithHomeEmpireWithFeedLine done


Status
 0      Errors,          1    Warning
 15000  Steps , 1.02 ms each,     Performance 138.479 MCells/s

 Energy estimate E  2.27671e-005 / max 1.97211e+001 / decrement   119 dB
 Energy estimate H  4.50222e-005 / max 1.69228e+001 / decrement   112 dB

 Time 00:18, 00:00 to go (estimated)
```

For CPW-RPA

```
This is ff V 5.40 (C) IMST GmbH 2002-2010

Phi is fixed, Phi= 0.0  Deg
Warning: switching off Mirror at zmin
Frequency f=5.500000000000000e+009 Hz
 Normalization:  Gain_Inc    Port 1

          Power into excitation port is P_in     = 9.848771888507194e-001
 Incident Power into excitation port is P_in_inc = 1.000000000000000e+000
          Radiated power              is P_rad    = 9.705142998980861e-001
 Excitation port is 1
 Antenna   Efficiency (P_rad/P_in)     is 98.542 %
 Radiation Efficiency (P_rad/P_in_inc) is 97.051 %
   Power at xmin is 1.135757723567282e-001 ( 11.703 %), IMAG -4.626000533356328e-003 (  -0.477 %)
   Power at xmax is 8.835585848375560e-002 (  9.104 %), IMAG 1.099005464852759e-002 (   1.132 %)
   Power at ymin is 1.729224495772800e-001 ( 17.818 %), IMAG 3.170221372326916e-004 (   0.033 %)
   Power at ymax is 1.653862581893112e-001 ( 17.041 %), IMAG 1.622600710241687e-003 (   0.167 %)
   Power at zmax is 4.302739612910111e-001 ( 44.335 %), IMAG 1.722360953722299e-002 (   1.775 %)
farfield processing: 100.00 % done.
***  Simulation  for BewThesisCPWPatchAntennaOnAug24 done
```

Status

```
0      Errors,          2    Warnings
10000  Steps , 1.74 ms each,     Performance 127.793 MCells/s

Energy estimate E  2.26320e-003 / max 2.11821e+001 / decrement    79 dB
Energy estimate H  3.66846e-003 / max 2.17146e+001 / decrement    75 dB

Time 00:22, 00:00 to go (estimated)
```

5.3 Summary of Simulation Results and Discussion

Table 5 *Simulation results of each antenna type.*

Antenna Type	*Maximum Return Loss (RL in dB)*	*Bandwidth (in MHz)*	*Number of Independent 20 MHz Channels*	*Directivity (in dB)*	*Gain (in dB)*
Conventional RMSA	***-22.71905***	***196.5776 (3.574%)***	***7***	***+7.187746***	***+7.037120***
Bandwidth-Enhanced RMSA	***-24.489329***	***315.341 (5.734%)***	***11***	***+7.472628***	***+7.463715***
CPW Rectangular-Patch Antenna	***-18.203675***	***384.2327 (6.986%)***	***13***	***+2.795113***	***+2.665129***

A. *When BW-enhanced RMSA compared with conventional RMSA*:

- It has got a bandwidth of ***315.341 MHz* (*5.734%*)**;
- That is, ***118.7655 MHz*** (or ***2.16%*)** more bandwidth from *conventional RMSA*;
- It has ***11*** independent 20 MHz channels (i.e., ***4 extra***);
- There is also a slight increment in gain, i.e.; by an amount of ***+0.426595 dB***. The reason is: as the patch width *W* increases, directivity *D* will also increase because there is a direct proportionality between *D* and *W* as shown in Eqn. (*2.5*). That is,

$$Directivity,\ D \cong 0.2W + 6.6 + 10\log\left(\frac{1.6}{\sqrt{\varepsilon_r}}\right)\ dB$$

B. Comparing CPW-RPA with the other two antennas:

- It has got a bandwidth of ***384.2327 MHz*** (***6.986%***);
- That is, ***187.6551 MHz*** (or ***3.412%***) and ***68.8917 MHz*** (or ***1.253%***) more bandwidth from *Conventional RMSA* and *BW-Enhanced RMSA*, respectively;
- It can accommodate ***13*** channels (i.e., ***6 more*** from *conventional RMSA* and ***2 more*** from *BW-Enhanced RMSA*);
- However, it has ***lower gain*** from the two *RMSAs*.

CHAPTER 6

Conclusion and Recommendations for Future Work

6.1 Conclusion

In this thesis, I have designed two aspects of microstrip antenna, that is, *conventional RMSA* and *BW*-enhanced *RMSA*. I have used "lowering Q_t of the antenna" as a bandwidth enhancement technique. This has been achieved by keeping the substrate ε_r at 2.2 and increasing the substrate height h and the patch width W, because Q_t has an inverse relationship with h and W. By doing so, I have achieved a bandwidth increment of ***118.7655 MHz*** (or ***2.16%*****)** for *BW-Enhanced RMSA* in comparison with *conventional RMSA*.

The other very important work in this thesis is to design a *CPW-RPA*. This antenna type has similar characteristics like microstrip antenna than loop antenna. Then, from the simulation result of *CPW-RPA* it is observed that *BW* increment of ***187.6551 MHz*** (or ***3.412%***) and ***68.8917 MHz*** (or ***1.253%***) from *conventional RMSA* and *BW- Enhanced RMSA*, respectively.

The challenging situations that I encountered in the design of *CPW-RPA* are: finding out the *CPW* feed line length, how to connect this feed line to the lumped port and where to terminate and so on. In addition, in the antenna design and simulation, maintaining of all the antenna parameters at the desired value, finding the exact feed point location for proper matching, and finding out the optimum Q_t value were another difficulties.

The data listed in Table 5 shows that *CPW-RPA* has better *BW* than the two *RMSAs*. Hence, it can accommodate more number of independent 20 MHz channels. However, the gain is lower than the two antennas; therefore, *CPW-RPA* covers *shorter range wave* so it is used for typical *WLAN* indoor application and as long as the base station is within the range the antenna can be in any orientation in the space.

6.2 Recommendations for Future Work

Based on gathered observations while doing this thesis; other techniques were identified which would benefit for further bandwidth enhancement. These are:

- Using reactive loading together with modification of the patch shape;
- Trapezoidal patch structure with *CPW* feeding slot;
- Using slits on the patch and etching slots in the ground plane, and so on.

In addition, *CPW* patch antenna *gain enhancement* is also another important research area for the future.

References

[1] Wikipedia the free encyclopedia, "List of WLAN Channels".

[2] Phil Belanger and Ken Biba, "Tutorials on 802,11n unlock the potential of the 5GHz Band", *www.wi-fiplanet.com*, August 9, 2007.

[3] Western Australian Telecommunications Research Institute, WATRI, "Wireless System and its Detail".

[4] Constantine A. Balanis, *Antenna Theory Analysis and Design*, 3rd ed. Hoboken, New Jersey: Wiley, 2005.

[5] Zhi Ning Chen and Michael Y. W. Chia, *Broadband Planar Antennas: Design and Application*. England: Wiley, 2006.

[6] Ramesh Garg, Prakash Bharita, Inder Bahl, and Apisak Ittipiboon, *Microstrip Antenna Design Handbook*. Norwood, MA: Artech House, 2001.

[7] Rajeev Bansal, *Handbook of Engineering Electromagnetics*. New York: Marcel Dekker, 2004.

[8] Y. T. Lo and S. W. Lee, *Antenna Handbook: Antenna Theory*, Vol. II. New York: Van Nostrand Reinhold, 1993.

[9] John Volakis, *Antenna Engineering Handbook*, 4th ed. New York: McGraw-Hill, 2007.

[10] Warren L. Stutzman and Gary A. Thiele, *Antenna Theory and Design.* New York: Wiley, 1981.

[11] J. R. James and P.S. Hall, *Handbook of Microstrip Antennas*. London, UK: Peter Peregrinus, 1989.

[12] Girish Kumar and K. P. Ray, *Broadband Microstrip Antennas.* Norwood, MA: Artech House, 2003.

[13] Kin-Lu Wong, *Compact and Broadband Microstrip Antennas*. New York: Wiley, 2002.

[14] Thomas A. Milligan, *Modern Antenna Design*, 2nd ed. Hoboken, New Jersey: Wiley, 2005.

[15] Kai Chang, *RF and Microwave Wireless Systems*. New York: Wiley, 2000.

[16] K. C. Gupta, Ramesh Garg, Inder Bahl, Prakash Bhartia, *Microstrip Lines and Slotlines,* 2nd ed. Norwood, MA: Artech House, 1996.

[17] Inder Bahl, *Lumped Elements for RF and Microwave Circuits*. Norwood, MA: Artech House, 2003.

[18] *EMPIRE™ XCcel User and Reference Manual for the 3D-EM field Time Domain Simulator.* Germany: IMST GmbH 1998-2010, Ver. 5.4, 2010.

[19] Adnan Kaya, Selcuk Kilinc, E. Yesim Yuksel, and Ugur Cam, "Bandwidth Enhancement of A Microstrip Antenna Using Negative Inductance As Impedance Matching Device," *Microwave Opt. Tech. Lett*, vol. 42, no. 6, pp. 476-478, Sep. 2004.

[20] RSA Raja Abdullah, D. Yoharaaj, and Alyani Ismail, "Bandwidth Enhancement Technique in Microstrip Antenna for Wireless Applications," *PIERS ONLINE*, vol. 2, no. 6, pp. 633-639, Nov. 2006.

[21] Wen-Ling Chen, Guang-Ming Wang, and Chen-Xin Zhang, "Bandwidth Enhancement of a Microstrip-Line-Fed Printed Wide-Slot Antenna With a Fractal-Shaped Slot," *IEEE Trans. Antennas Propagat.*, vol. 57, no. 7, pp. 2176-2179, Jul. 2009.

[22] David R. Jackson and Nicolaos G. Alexopoulos, "Simple Approximate Formulas for Input Resistance, Bandwidth, and Efficiency of a Resonant Rectangular Patch," *IEEE Trans. Antennas Propagat.*, vol. 39, no. 3, pp. 407-410, Mar. 1991.

[23] Rainee N. Simons, *Coplanar Waveguide Circuits, Components, and Systems*. New York: Wiley, 2001.

[24] Ingo Wolff, *Coplanar Microwave Integrated Circuits*. Hoboken, New Jersey: Wiley, 2006.

[25] Peter Russer, *Electromagnetics, Microwave Circuit and Antenna Design for Communications Engineering*, 2nd ed. Norwood, MA: Artech House, 2006.

[26] Hubregt J. Visser, *Approximate Antenna Analysis for CAD*. UK: Wiley, 2009.

[27] T. C. Edwards, M. B. Steer, *Foundations of Interconnect and Microstrip Design*, 3rd ed. England: Wiley, 2000.

[28] R. Hoffmann, *Microwave Integrated Circuit Handbook*. Norwood, MA: Artech House, 1985.

[29] Franco Di Paolo, *Networks and Devices Using Planar Transmission Lines*. Boca Raton, Florida: CRC Press LLC, 2000.

[30] K. Li, C. H. Cheng, T. Matsui and M. Izutsu, "Coplanar Patch Antennas: Principle, Simulation and Experiment," *IEEE paper*, pp. 402-405, 2001.

[31] K. Li, C. H. Cheng, T. Matsui and M. Izutsu, "Electric Field in Coplanar Patch Antennas (CPA): Simulation and Measurement," *IEEE paper*, 2005.

[32] Celal Yildiz and Mustafa Turkmen, "Synthesis formulas for Conductor-Backed Coplanar Waveguide," *Microwave Opt. Tech. Lett*, vol. 50, no. 4, pp. 1115-1117, 2008.

[33] Robert A. Sainati, *CAD of Microstrip Antennas for Wireless Application*. Norwood MA: Artech House, 1996.

[34] K. F. Tong, K. Li, T. Matsui, and M. Izutsu, "Broad-Band Double-Layered Coplanar Patch Antennas With Adjustable CPW Feeding Structure," *IEEE Trans*. *Antennas Propagat*., vol. 52, no. 11, pp. 3153-3156, Nov. 2004.

Acknowledgements

The accomplishment of this thesis work would be impossible without people who supported me and believed in me throughout my study.

I would like to express my sincere gratitude and thanks to Dr.-Ing. Mohammed Abdo, my advisor, for his encouragement, invaluable guidance and discussions. His endless support, advice and timely suggestion guided me to the completion of this thesis work.

I would like to thank Ato Teshome Hambissa, the lab assistant, for providing an excellent working environment. Thanks also extend to my friends and especially my classmates for all the discussions we had and the experience we shared. I have enjoyed their companionship so much during my study.

It is also my pleasure to thank my brother, Zena Bekele, for his support and encouragement all the time.

Last but not least, I would like to express my appreciation and special thanks to Zerthun Hailu, my wife, who taught me the value of hard work by her own example. She provided me her unlimited love and enormous support during those difficult and challenging years.

Table of Contents

List of Tables

List of Abbreviations

2D/3D	-	*Two/Three Dimension*
BW	-	*Bandwidth*
CPW	-	*Coplanar Waveguide*
CPWA	-	*Coplanar Waveguide Antenna*
CPW-RPA	-	*Coplanar Waveguide Rectangular-Patch Antenna*
DCS	-	*Digital Communication System*
FDTD	-	*Finite Difference Time Domain*
FWM	-	*Full-Wave Methods*
GSM	-	*Global System for Mobile*
MMIC	-	*Monolithic Microwave Integrated Circuit*
MSA	-	*Microstrip Antenna*
PCS	-	*Personal Communication System*
PIER	-	*Progress In Electromagnetics Research*
QSM	-	*Quasi-Static approximation Methods*
RCA	-	*Radio Corporation of America*
RF	-	*Radio Frequency*
RL	-	*Return Loss*
RMSA	-	*Rectangular-Patch Microstrip Antenna*
TEM	-	*Transverse Electromagnetic*
TL	-	*Transmission Line*
TM	-	*Transverse Magnetic*
UMTS	-	*Universal Mobile Telecommunication System*
VSWR	-	*Voltage Standing Wave Ratio*
WLAN	-	*Wireless Local Area Network*

List of Figures

Abstract

These days, there is a very large demand for wireless applications because of its mobility, the demand for high speed transmission of large data, customer request for multi-media service, and the need for new technologies, and so on. Those systems require small size and high performance components. Antenna is one of the key elements to establish communication link and cover wide frequency range. In this thesis, the wireless application that has been selected to be studied is Wireless Local Area Network (*WLAN*) operating at 5 GHz frequency range based on *IEEE 802.11n* standard.

Antennas that are used in *WLAN* application should be low profile, light weight, low volume and broad bandwidth. *MSA* and CPW antennas suit the aforementioned features with the exception of their narrow bandwidth and lower gain limitations.

In this thesis, conventional *RMSA* operating at resonant frequency of 5.5 GHz has been initially designed. A substrate material with low permittivity (i.e.; ε_r = 2.2) namely *RT/Duroid 5880* is used as the dielectric for the radiating patch. The simulation was carried out using *EMPIRE*^{TM} *XCcel* software of version 5.4. From the simulation result, a *BW* of ***196.5776 MHz*** (i.e.; ***3.574%***) and a gain of ***+7.0604 dB*** have been obtained. This design has been used as a benchmark for the design of *BW*-Enhanced *RMSA* by using "lowering the total quality factor (Q_t)" as a bandwidth enhancement technique. Lowering Q_t has been achieved by increasing the patch width, *W*, and the substrate height, *h*. By using this technique, a BW of ***315.3431 MHz*** (i.e.; ***5.734%***) and a gain of ***+7.463715 dB*** have been achieved. Finally, a *CPW-RPA*, with the same resonant frequency and dielectric constant, has been designed. Then, from the simulation result a bandwidth of ***384.2327 MHz*** (i.e., ***6.986%***) and a gain of ***+2.665129 dB*** have been obtained.

Key words: *microstrip antenna; coplanar waveguide antenna; VSWR; return loss; Q_t - factor; bandwidth; gain.*